Controller Design For Unity Power Factor Supply To Induction Motor Drive

Major Thesis Submitted In Partial Fulfillment of The Requirements

for Award of the Degree of

MASTER OF TECHNOLOGY

IN

CONTROL AND INSTRUMENTATION (C&I)

SUBMITTED BY

Rohit Goyal
(2K11/C&I/10)

Under The Esteemed Guidance of

Prof. Pramod Kumar **&** **Mrs. Priya Mahajan**

DEPARTMENT OF ELECTRICAL ENGINEERING

DELHI TECHNOLOGICAL UNIVERSITY

BAWANA ROAD, DELHI-110042

2013

DELHI TECHNOLOGICAL UNIVERSITY

DEPARTMENT OF ELECTRICAL ENGINEERING

CERTIFICATE

This is to certify that the thesis entitled, "**Controller Design For Unity Power Factor Supply To Induction Motor Drive**" has been submitted in partial fulfillment of the requirements for award of the degree in M.Tech in Electrical Engineering (Control & Instrumentation) under our supervision by **Rohit Goyal** (2K11/C&I/10), at the Delhi Technological University.

This work has not been submitted earlier in any university or institute for the award of any degree to the best of our knowledge.

Prof. Pramod Kumar

Mrs. Priya Mahajan
Assistant Professor
Department of Electrical Engineering
Delhi Technological University

Prof. Madhusudan Singh
Head Of the Department
Dept. of Electrical Engineering
Delhi Technological University

Acknowledgement

I am grateful to Prof. Pramod Kumar and Mrs. Priya Mahajan, Department of Electrical Engineering, Delhi Technological University, New Delhi for providing me the opportunity to undertake the project and under whom I worked and who were a source of inspiration throughout the whole period. Also, the interrogations frequently executed by them refined my knowledge about the subject and acted as the platform for my development. This report is a superstructure over the guidelines, directive advices and creative suggestions provided by them as the substructure.

I sincerely thank them for solving my queries and making me able to have vision and penetration. Last but not the least, I would be failing in my duties if I forget to convey my thankful regards to all the members of staff of the department whom I came in contact with and who, in some way or another, were helpful and supporting me.

Rohit Goyal
(2K11/C&I/10)

Abstract

Induction motors are widely used in industry and agriculture pumps due to the fact that they are relatively cheap, rugged and maintenance free. However, they need reactive power for its operation. Thus, a large reactive power is required to be supplied and transmitted by the supply to the load. Inorder to improve efficiency of transmission lines as well as efficiency of induction motor, it is desired to improve the power factor by reducing the reactive power requirement. This can be done using upf controller which uses SPWM technique. In the present work, unity power factor on the supply side is obtained using sinusoidal pulse width modulation.

Further, vector control for the control of speed of induction motor is used in the present study, which has widespread use in high performance induction motor drives. It allows, by means of a co-ordinate transformation, decoupling of the electromagnetic torque from the rotor flux. The decoupling control between the flux and torque allows induction motor to achieve fast transient response. Therefore, it is used in high performance motor applications. In the present work, an indirect vector control scheme is implimented with hysteresis current controller.

List of Symbols used

f	Frequency (Hz)
I_f	Machine field current.
I_s	Rms stator current.
i_{dr}^{s}	d^s axis rotor current
i_{ds}^{s}	d^s axis stator current
i_{qr}	q^e - axis rotor current
i_{qs}	q^e - axis stator current
L_m	Magnetizing inductance
L_r	Rotor inductance
L_s	Stator inductance
L_{lr}	Rotor leakage inductance
L_{ls}	Stator leakage inductance
L_{dm}	d^e- axis magnetizing inductance
L_{qm}	q^e axis magnetizing inductance
N_e	Synchronous speed (rpm)
N_r	Rotor speed
P	Number of poles
S	Slip
T_e	Developed torque
V_{dc}	DC voltage
φ_{dr}^{s}	d^s- axis rotor flux linkage
φ_{ds}^{s}	d^s- axis stator flux linkage
φ_{qr}	q^e - axis rotor flux linkage
φ_{qs}	q^e- axis stator flux linkage
ω_e	Stator or line frequency (r/s) Rotor mechanical speed
ω_r	Rotor electrical speed
ω_{sl}	Slip frequency
R_s	Stator Resistance
R_r	Rotor Resistance

List of Figures

Figure 1	IGBT PWM rectifier/inverter system
Figure 3.1	Block diagram of unity power factor control of induction motor drive
Figure 3.2	Single Phase Bridge, Voltage Source PWM Converter
Figure 3.3	Block Diagram of Unity Power Factor Converter Control
Figure 3.4	Phasor Diagram of Front End Converter: a.)Unity Power Factor forward power flow, b.) Unity Power Factor Reverse power flow
Figure 3.5	Equivalent circuit of an induction motor in the synchronous rotating reference frame, a) q-axis circuit b) d-axis circuit
Figure 3.6	Block diagram current hysteresis controller
Figure 3.7	Fixed band shape of hysteresis controller
Figure 4.1	Shows the various simulink block of induction motor drive
Figure 4.2	Hysteresis Current Regulator-simulink model
Figure 4.3	Universal Bridge block
Figure 4.4	Flux Calculation Simulink Block
Figure 4.5	Theta Calculation Simulink block
Figure 4.6	d-q to abc transformation Simulink blocks
Figure 4.7	abc to d-q Transformation Simulink Blocks
Figure 4.8	Proportional Integral Controller block diagram
Figure 4.9	Unity power factor Simulink block
Figure 5.1	Implementation of unity power factor control of induction machine
Figure 5.2(a) & (b)	Simulink plot showing supply side unity power factor control on “no load” at 60 rad/sec
Figure 5.3	Simulink plot showing voltage(line-line), three phase stator current, speed and electromagnetic torque on no load at 60rad/sec speed
Figure 5.4(a) & (b)	Simulink plot showing supply side unity power factor control on “full load” at 60 rad/sec

Figure 5.5	Simulink plot showing voltage(line-line), three phase stator current, speed and electromagnetic torque on full load at 60rad/sec speed
Figure 5.6(a) & (b)	Simulink plot showing supply side unity power factor control on “no load” at 150 rad/sec
Figure 5.7	Simulink plot showing voltage(line-line), three phase stator current, speed and electromagnetic torque on no load at 150rad/sec speed
Figure 5.8(a) & (b)	Simulink plot showing supply side unity power factor control on “full load” at 140 rad/sec
Figure 5.9	Simulink plot showing voltage(line-line), three phase stator current, speed and electromagnetic torque on full load at 140rad/sec speed
Figure 5.10(a) &(b)	Simulink plot showing supply side unity power factor control on “no load” at 140 rad/sec for high rating motor
Figure 5.11	Simulink plot showing three phase stator current, speed and electromagnetic torque on no load at 140rad/sec speed for high rating motor

Table of Contents

Certificate II

Acknowledgement III

Abstract IV

List of Symbols Used V

List of Figures VI

Chapter 1: Introduction

1.1 Introduction 2

1.2 Motivation of work 4

1.3 Outline of thesis 5

1.4 Conclusion 5

Chapter 2: Literature Review

2.1 Introduction 7

2.2 Supply Side Unity Power Factor Control 7

2.3 Indirect Vector Control Of Induction Motor 10

2.4 Conclusion 12

Chapter 3: Implementation Of Unity Power Factor And Vector control of Induction Motor

3.1 Introduction 14

3.2. Induction Motor Drive System 14

3.2.1 Power Factor Control Via PWM Converter 15

3.2.2 Steady State Design Considerations 17

3.3 Dynamic Model of Induction Motor 19

3.4 Vector Control Methodology 21

3.4.1 Control Algorithm 21

3.4.2 abc-dq Transformation 22
3.5 Hysteresis Current Algorithm 23
3.6 Conclusion 24

Chapter 4: Controller Design Using Simulink
4.1 Introduction 26
4.2 Simulink Model Of Induction Motor Drive 26
4.2.1 Simulink Model Of Hysteresis Current Regulator 27
4.2.2 Universal Bridge 27
4.2.3 Flux Calculation Simulink Model 28
4.2.4 Theta Calculation Simulink Model 29
4.2.5 d-q to abc Transformation Simulink Model 29
4.2.6 abc to d-q Transformation Simulink Model 30
4.2.7 PI Controller 30
4.3 Unity Power Factor Control Block 31
4.4 Conclusion 31

Chapter 5: Simulation Results
5.1 Introduction 33
5.2 Implementation In Matlab 33
5.3 Simulink Results 35
5.4 Results Analysis 46
5.5 Conclusion 47

Chapter 6: Conclusion and Further Scope
6.1 Conclusion 49
6.2 Future Scope 49

References 51

Chapter 1

Introduction

Introduction

Electric drives for motion control must have a four quadrant operation capability, fast torque response, and controllability of speed and torque over a wide range of operating conditions. A separately excited dc motor had been the most popular choice for many industrial drives because it provides direct control of the magnitude of armature current and, in proportion, the torque, in spite of its inherent drawback of the expensive, bulky and maintenance-prone commutator. On the other hand induction motors with their less expensive, simple and more robust structures are more suitable for industrial environments though their control is quite complex. This is due to the fact that the rotor current in an induction motor which is responsible for the torque production owes its origin to the stator current which also contributes to the air-gap flux resulting in a coupling between the torque and flux producing mechanism. In the dc machine, the armature current control the torque and the field current in the stationary poles produces the magnetizing flux are independently accessible. Moreover, for a fully compensated dc motor, the spatial angle between the flux and the armature mmf is held at 90° with respect to each other, independent of the load, by the commutator and the brushes whereas in an ac motor (both induction and synchronous), the spatial angle between the rotating stator and rotor fields varies with the load and gives rise to oscillatory dynamic response. Now a days, with the advent of new power electronics based control, the emphasis is to find new control methods for ac motors that emulate the dc motor control by orienting the stator current so as to attain independent and 'decoupled' control of flux and torque which is also known as 'field orientation' control. This require control of both the magnitude and phase of ac quantities and thus are referred to as 'vector control methods'.

This control can be achieved using IGBT based power converters. This ac-dc-ac power converter comprises of two major parts:

a.) The ac to dc converter

b.) The dc to ac inverter

For the development of ac to dc converter and dc to ac inverter systems of the induction motor drive advanced techniques have been applied. This includes the

implementation of unity power factor control and three level current hysteresis PWM switching is applied to the inverter. The converter carries out PWM control, making it possible to make the phase difference between the primary voltage and current of the supply side a zero. In other words, unity power factor can be obtained and the supply line harmonics are lowered. This guarantee a compatibility between the ac supply and the converter, which will lead to reduce vibration, power losses, noise in the main ac supply, high performance in terms of efficiency and harmonic control.

Inverters of high switching frequency are suitable for ac drives since they operate the drives in current control mode and practically sinusoidal stator current for high dynamic performance. In addition the switching frequencies of the order of 20 kHz reduced audible noises. Now a days, insulated-gate-bipolar transistors (IGBT's) have been used, it require very little gate drive power and offer low on resistance. An IGBT possesses high input impedance like a MOSFET and has low on-state power loss as in a BJT.

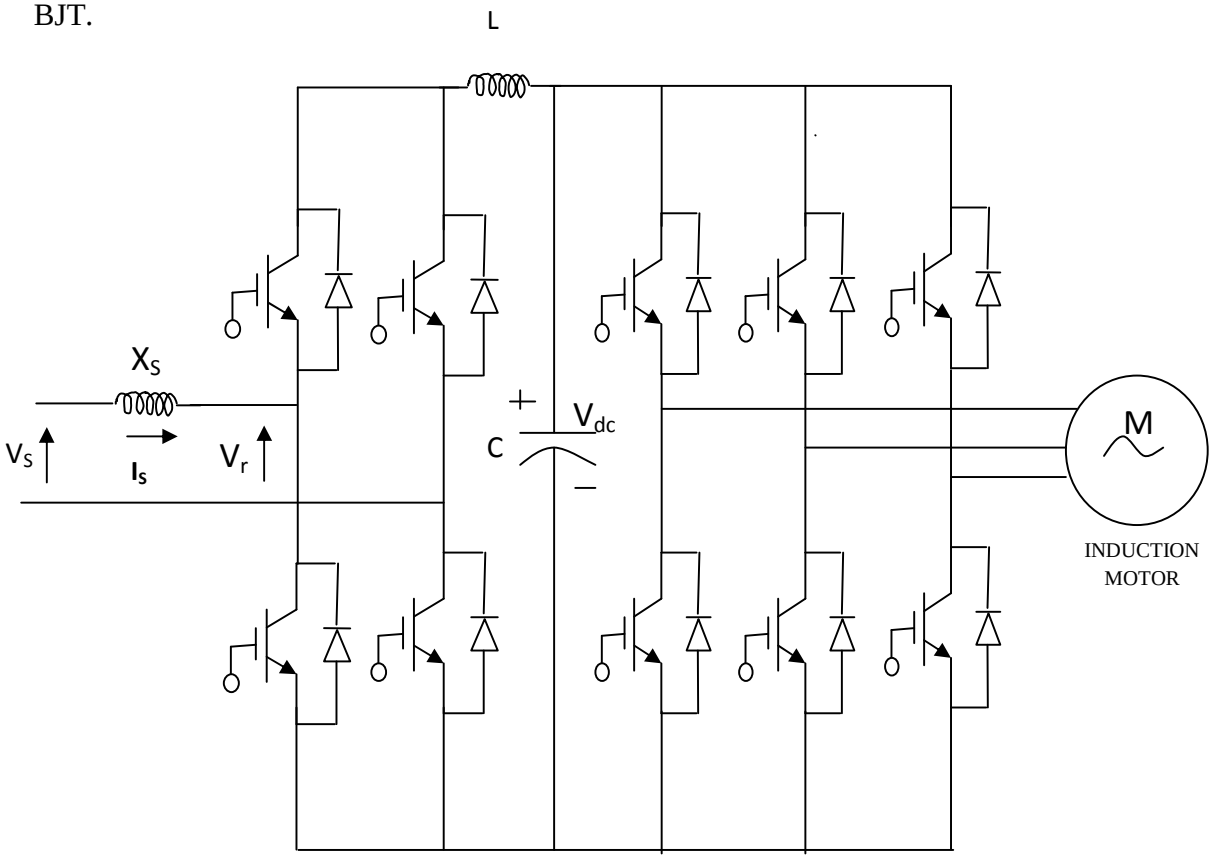

Figure 1 IGBT PWM rectifier/inverter system

The front-end ac to dc PWM converter feeding a dc to ac PWM inverter, takes near sinusoidal current at unity power factor from the ac mains, and should have bidirectional power flow capability. An ac to dc PWM front-end converter with a reactor at the single-phase supply side convenes all the necessities and is also used as a voltage source for dc to ac PWM inverters driving induction motors. The induction motor drive system is shown in Figure 1. The front-end for the system is a full-bridge IGBT PWM converter with an ac reactor. The motor side converter is a high switching frequency IGBT three phase PWM inverter. The entire system controls from single-phase mains supply.

Apart from above mention part, the electric drives also comprises of the control part that comprises of the controller circuit. This system gives many beneficial features such as ease of maintenance due to contact-less circuits, brushless motors, compactness, lighter weight, high performance, high reliability and lower cost as a result of which this ac drive system is advantageous for the powering and driving of induction motor.

1.2 Motivation of Work

The field of ac drives especially induction motor drives has experienced an explosive growth in recent years. Induction motor drives have been the workhouses in industry for variable speed application in a wide power range that covers from fractional horsepower to multi megawatts. These applications includes pumps and fans, paper and textile mills, subway and locomotive propulsion, machine tools and robotics, electric and hybrid vehicles, home appliances, heat pumps and air conditioners, rolling mills, wind generation system, etc. The control and estimation of induction motor drives constitute a vast area under discussion and the technology has further advanced in recent years. In addition to process control, the energy saving aspects of variable frequency drives is getting a lot of attention nowadays.

Motivation of work is to maintain supply side power factor unity for induction motor drive as well as speed control of 3 phase induction motor by indirect field oriented control using current hysteresis PWM switching of inverter.

1.3 Outline Of Thesis

The whole work of dissertation is organized in 6 chapters.

Chapter 1 presents the general introduction of induction motor, IGBT PWM rectifier/inverter system and motivation of work.

Chapter 2 contains the literature review of the thesis for supply side unity power factor control and indirect vector control of induction motor.

Chapter 3 contains the induction motor drive system followed by power factor control and design consideration of converter. The dynamic modeling of induction motor and its vector control methodology is also explained in this chapter.

Chapter 4 contains simulink model for controller design for unity power factor supply to induction motor drive. Different control blocks are explained in this chapter.

Chapter 5 contains the simulink results. The results are presented and analysed in this chapter.

Chapter 6 contains the conclusions based on the simulink results. It also includes the further improvements in controllers such as design of active power filters to minimize the harmonics.

1.4 Conclusion

In this chapter induction motor drives has been introduced. The motivation of work and outline of thesis is also discussed.

Chapter 2

Literature Review

Introduction

Induction motor drives comprises of transmission lines, transformer, switchgear and induction motor system. The induction motor system draw reactive power considerably from the supply, this results in poor power factor which in turn draw more current. This reduces the capacity of transformer and transmission lines and efficiency of overall system is also reduces, thus there is need to improve the power factor of induction motor drives. A brief literature review relative to enhancing the power factor of induction motor has been presented in this chapter without exhaustive presentation.

Mainly the following areas are covered:

(a) Supply side unity power factor control

(b) Indirect vector control of induction motor

2.2 Supply Side Unity Power Factor Control

K. Thiyagarajah, V. T. Ranganathan [1] described an inverter/converter system operating from a single- phase supply. The power device used in the system is the IGBT. The inverter can operate at switching frequencies up to 20 kHz. Snubber circuits along with energy recovery networks suitable for high frequency operation and experimental results from a laboratory inverter have been presented. The steady-state design considerations of the front-end converter have been discussed. The block diagrams for dynamic control in a rotating as well as a stationary reference frame have been developed. Experimental results from a laboratory converter with stationary reference frame control have been presented in support of the analysis The front end for the system is a regenerative single phase full-bridge IGBT converter along with an ac reactor. Steady-state design considerations and control techniques for unity power factor operation and fast current control of the front end converter in a rotating as well as stationary reference frame are discussed and compared.

Adrian David Cheok, Shoichi Kawamoto, Takeo Matsumoto, and Hideo Obi [2] described new developments in the design of high-speed electric trains with particular reference to the induction motor drive system. Advanced control techniques lead to a unity power factor seen by the ac supply as well as minimizing the power loss, line

harmonics, motor torque ripple and audible noise. By using advanced ac drive systems the developed high speed train offers high level efficiency, performance and passenger comfort. In addition unity power factor is presented to the ac catenary which maximizes the system efficiency and utilization.

P. Enjeti and A. Rahman [3] proposed a new single-phase to three-phase converter topology. The proposed converter is capable of powering a three-phase adjustable-speed ac motor drive from a single phase ac main while maintaining sinusoidal input current at near unity power factor. The proposed topology thus realizes the following features: It employs only six switches. It draws near sinusoidal current from the ac mains at close to unity power factor. It permits bidirectional power flow and, hence, facilitates regenerative braking. Suitable design equations are given for the proposed topology.

J. Itoh and K. Fujita [4] proposed two novel single-phase input to three-phase output converters which use the neutral point of the three-phase load. The feature of those circuits is to drain the power supply current to the motor as a zero-phase sequence current. The proposed circuits have the significant advantages of avoiding the use of additional reactive components and reducing the number of switching devices with respect to conventional circuits. Future efforts will be made for improving the performances of the proposed converters as follows:

- Optimization of the PWM method.
- Design of a special motor having accessible neutral point and small stator resistance.
- Compensation of the motor phase current distortion due to the inverter dead-time.

B. K. Lee, B. Fahimi and M. Ehsani [5] developed various reduced parts converter topologies and control strategies for power factor correction and motor control. From this investigation, the converter topologies could be mainly categorized into cascade type and unified type. The detailed operational principles and the performance comparison is to illustrate merits and limitations of the converters.

C. B. Jacobina, M. B. de R. Correa, A. M. N. Lima, and E. R. C. da Silva [6] has presented two reduced-switch-count ac drive systems for two-phase and three-phase motors. The converters implement both the input rectifier and the inverter by sharing a

leg to reduce the switch count as compared to the ten-switch configuration. It has been shown that the overall performance of these topologies is superior to the configurations using the dc-bus midpoint connection (six-switch converter). This happens because the THD is smaller, the voltage capability of the input and output converters can be controlled, and no ac fundamental current flows through the dc-bus capacitor.

R. Q. Machado, S. Buso, and J. A. Pomilio [7] described a single-phase to three-phase converter. The objective of feeding a three-phase induction motor is the main concern for such conversion. Due to the evolution of the farm technology, some of the local loads (as communication equipments, computers, electronic power converters etc) required high power quality that is anticipated as sinusoidal, symmetrical and balanced three-phase voltage. Additionally, to maximize the power from the feeder, the system provides a unity power factor to the grid. A three-phase voltage source pulse width modulation converter is used for this purpose. The power converter processes a fraction of the load power to regulate the dc voltage.

R. Q. Machado, S. Buso, and J. A. Pomilio [8] have presented the methodology for the analysis and control of a high-performance induction motor drive actuated by two controlled rectifier–inverter systems with reduced count of switching devices. The general approach for determining the modulation signals required for the carrier-based PWM pulse generation for this class of minimalist converters has been set forth. The input supply voltage is a single phase and the input current is controlled using a natural reference frame controller to operate close to unity displacement power factor. The nature of the modulation signals, the achievable motor dynamics, and waveforms are clearly lay out in simulation and experimental results. Compared with the conventional high-performance rectifier–converter motor drive system which has eight controllable switching devices, the converter systems studied in this paper has the same dynamic performance potential.

J. R. Rodrıguez, J. W. Dixon, J. R. Espinoza, J. Pontt, and P. Lezana [9] have reviewed the most important topologies and control schemes used to obtain ac–dc conversion with bidirectional power flow and very high power factor, each topology has advantages and disadvantages. Voltage-source PWM regenerative rectifiers have shown a tremendous development from single-phase low-power supplies up to high-power

multilevel units. Current-source PWM regenerative rectifiers are conceptually possible and with few applications in dc motor drives. The main field of application of this topology is the line-side converter of medium voltage CSI. Especially single-phase PWM regenerative rectifiers are the standard solution in modern ac locomotives. The control methods developed for this application allow for an effective control of input and output current and voltages.

D.-C. Lee and Y.-S. Kim [10] proposed a novel control scheme of single phase-to-three-phase pulse width-modulation (PWM) converters for low-power three-phase induction motor drives, where a single- phase half-bridge PWM rectifier and a two-leg inverter are used. With this converter topology, the number of switching devices is reduced to six from ten in the case of full-bridge rectifier and three-leg inverter systems. In addition, the source voltage sensor is eliminated with a state observer, which controls the deviation between the model current and the system current to be zero. A simple scalar voltage modulation method is used for a two-leg inverter, and a new technique to eliminate the effect of the dc-link voltage ripple on the inverter output current is proposed. Although the converter topology itself is of lower cost than the conventional one, it retains the same functions such as sinusoidal input current, unity power factor, dc-link voltage control, bidirectional power flow, and variable-voltage and variable-frequency output voltage.

2.3 Indirect Vector Control Of Induction Motor

The vector control technique has been widely employed in several electric drive applications . By providing decoupling of torque and flux control commands, the vector control can navigate an AC motor drive similar to a separately excited DC motor drive without sacrificing the quality of the dynamic performance.

There are essentially two ways of vector control method to apply to induction motor drive

(a) Direct or feed- back vector control of induction motor

(b) Indirect or feedforward vector control of induction motor

In direct Field orientation control the angle is obtained by the terminal voltages & currents, while as in indirect Field orientation control, the angle is obtained by using rotor position measurement & machine parameter estimation.

Early conceptual works in direct vector control were by Blaschke (1972) [11]and and the other, known as the indirect or feedforward method was invented by Hasse (1969)[12], [14] which were translated into practical implementation later by Gabriel *et al* (1980), Leonhard(1985) and many others with the advances in microprocessors and microcomputers along with power electronics. Now, it has been established as a powerful technique in the field of *ac* motor drives and adopted worldwide. Work has continued unabated in this field and several issues like simplification of practical system with advanced microprocessors, design of current regulators/flux observers, reliability enhancement, performance improvement, parameter adaptation etc. are still attracting the researchers in this field.

Field orientation has emerged as a powerful tool for controlling ac machines such as inverter-supplied induction motors. The dynamics performance of such a drive is comparable to that of a converter fed four quadrant dc drives. The complex functions required by field oriented control may be executed by microprocessors on line, thus greatly reducing the necessary control hardware.[13], [16]

An important requirement to obtain good control performance is to make the motor parameters in the field-oriented controller coincide with the actual parameters of the motor. The ability to inject currents into the motor with a current source opened up new possibilities for parameter determination. It was Takayoshi [14] who described a new identification technique utilizing injected negative sequence components. It is shown that the stator as well as rotor resistance and leakage inductance can be determined on line while the motor is driving the load. The theory is verified with a full-scale hybrid computer simulation of a field-oriented controlled PWM inverter, induction motor drive.

The performance of induction motor drive is mainly determined by the gating Pulses feeding the inverter. A current control technique using hysteresis [15], [19] can be applied for determining the pulse pattern. With this method, fast response current loop will be obtained and knowledge of load parameter is not required. However this method can cause variable switching frequency of inverter and produce undesirable harmonic generation. A new Space vector current control technique, proposed by Ting–Yu et.al.[20], for induction motor drive, shows better performance. No time-varying coordinate transformation and no complicated calculation are required. It is seen that

even a simple 8751 microcomputer can be used to implement a high-performance drive system. In addition, the proposed space vector-based current controller uses the extra information of error derivative to reduce the switching frequency greatly.

2.4 Conclusion

A brief literature review has been done on supply side unity power factor and indirect indirect vector control of 3 phase induction motor drives. A new single-phase to three-phase converter topology has been reviewed. The converter is capable of powering a three-phase adjustable-speed ac motor drive from a single phase ac main while maintaining sinusoidal input current at near unity power factor.

Indirect vector control provides decoupled control of the rotor flux magnitude and the torque-producing current, with a fast, near-step change in torque. The fast torque response is achieved by estimating, measuring, or calculating the magnitude and position of the rotor flux in the machine. In this method the calculation of the rotor flux position is dependent on the rotor resistance value.

Chapter 3

Implementation of Unity Power Factor and Vector control of Induction Motor

Introduction

Induction motor has a tendency to work at low power factor particularly under light load conditions. This may leads to a low effectiveness in drawing power from the mains supply, and will require that the current drawn for the same power is higher. This increases the volt-ampere requirement of the power drive components, and the mains supply. To minimize the line current, power loss and motor torque ripple, induction motor drives along with unity power factor control on supply side are preferred. Power factor correction provides many additional benefits such as it reduces the line harmonics, increase system capacity, improves the voltage and reduces the heat losses.

3.2. Induction Motor Drive System

The block diagram of an induction motor drive is as shown in Figure 3.1**.**

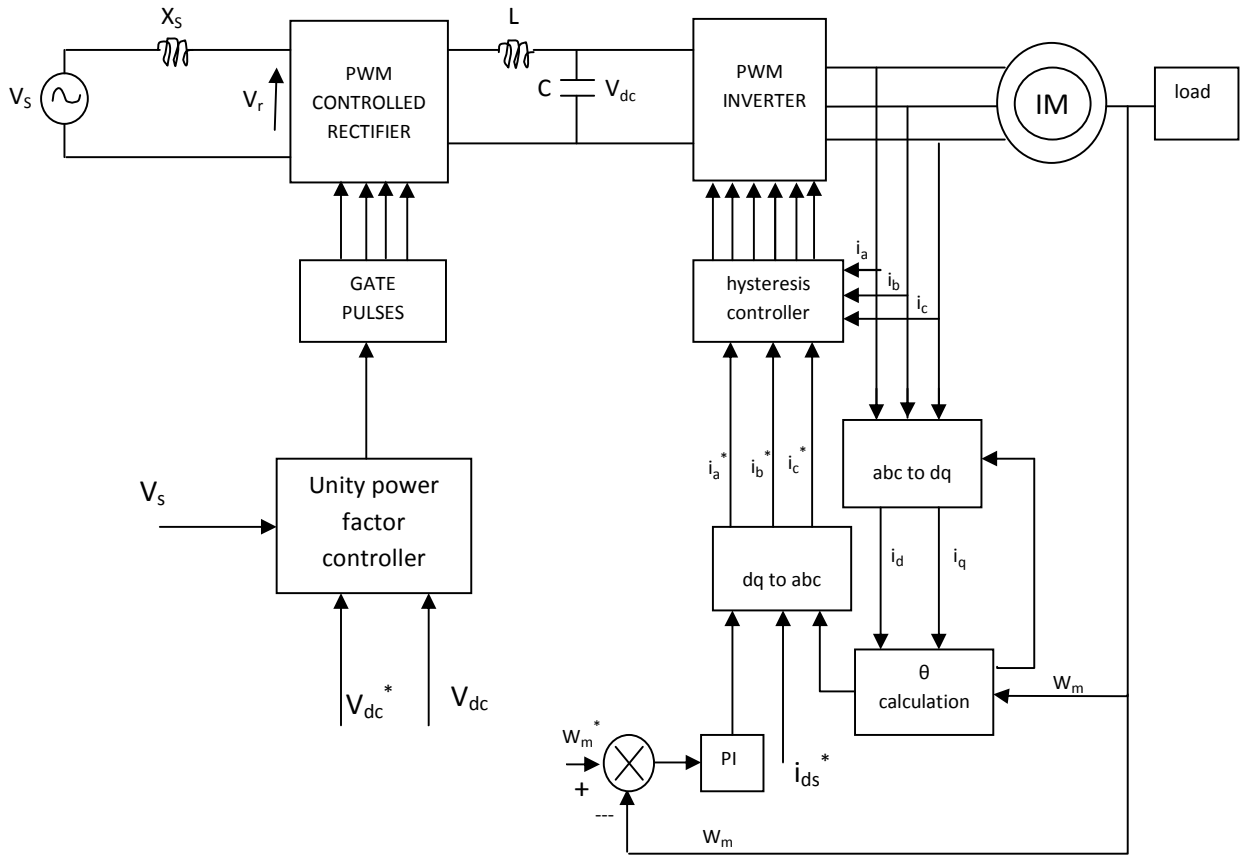

Figure 3.1 Block diagram of unity power factor control of induction motor drive

In this system, the 3 phase induction motor is supplied with single phase ac power supply. This ac supply is connected to a four-quadrant ac to dc switched mode converter. The dc link is connected to an inverter, which in turn supply induction motor. The supply line voltage is applied to the ac-dc-ac power converter circuit. The output of the ac-dc converters is connected to the dc bus, the dc link is connected to the dc-ac three level inverter.

3.2.1 Power Factor Control Via PWM Converter

The controlled rectifier as used in earlier times comprises of conventional thyristors, natural commutation from the ac supply, and phase angle firing delay control. This resulted in ac currents that are both distorted and lag the voltage. The non-sinusoidal nature of the currents and the poor power factor cause numerous problems to the ac supply power system of the electricity generating and distribution companies.

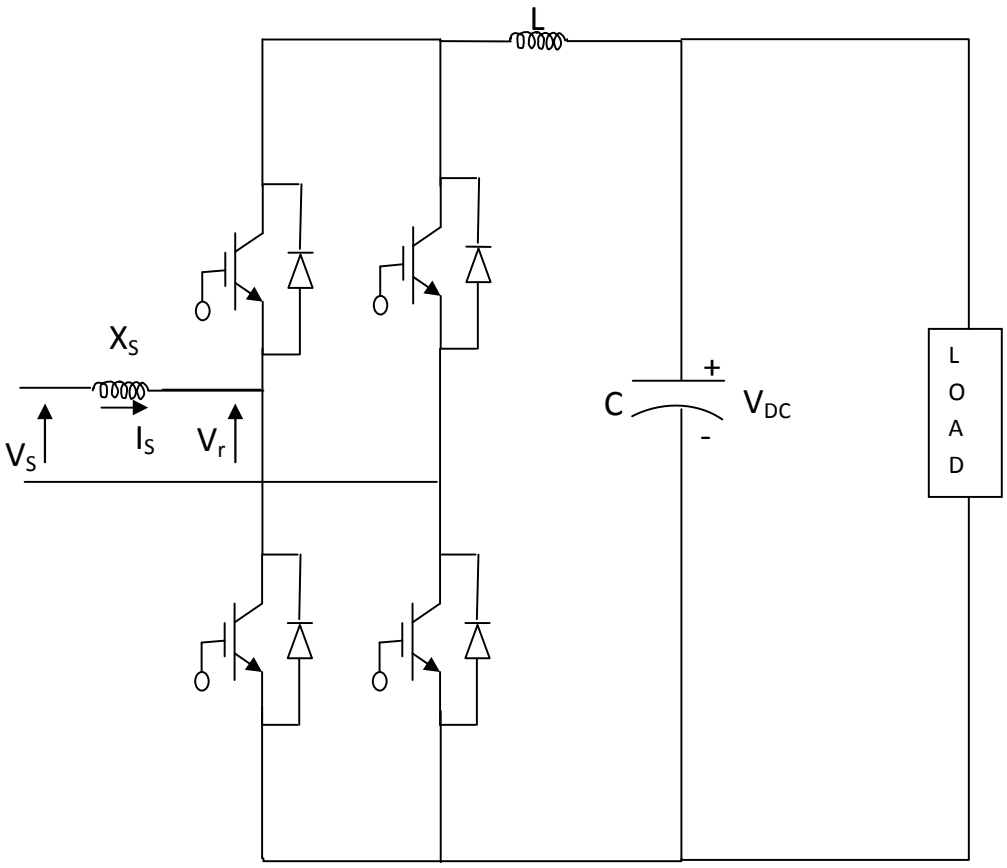

Figure 3.2 Single Phase Bridge, Voltage Source PWM Converter

A controlled converter which takes near sinusoidal current at near unity power factor is the ideal. Such a converter is possible using fast switching device and a control strategy known as pulse width modulation (PWM). One of the possible switching devices which can be turned off from the base or gate is the insulated gate bipolar transistor (IGBT). The basic circuit configuration for the converter is shown in Figure 3.2 where the essential components of the voltage-sourced PWM converter are shown. Each arm of the converter consists of a diode with an inverse parallel connected switching device and the insulated gate bipolar transistor (IGBT). An inductor of reactance X_s is included in series with the ac supply. Here inductor(X_s) is used to maintain the supply side power factor unity as explained in 3.2.2

In order to improve the power factor of the ac supply, a unity power factor control scheme has been implemented for the induction drive. To achieve this, real time control of the converter voltage with current and voltage feedback is used, which controls the phase difference between the ac supply voltage and current. It can be easily derived that in the unity power factor case, the converter voltage amplitude is:

$$V_r = \sqrt{V_s^2 + (I_s X_s)^2} \tag{3.1}$$

Here,

V_s = Source voltage amplitude (peak value)

I_s = Input current (peak value)

V_r = Converter voltage amplitude

If the converter voltage can be controlled to the above value then unity power factor will be maintained. In the developed upf controller, a control system is used to maintain unity power factor by controlling the switching of converter. The upf controller maintains a constant dc output voltage, in order that a steady dc link voltage is fed to the inverter. The block diagram of the controller can be seen in Figure 3.3.

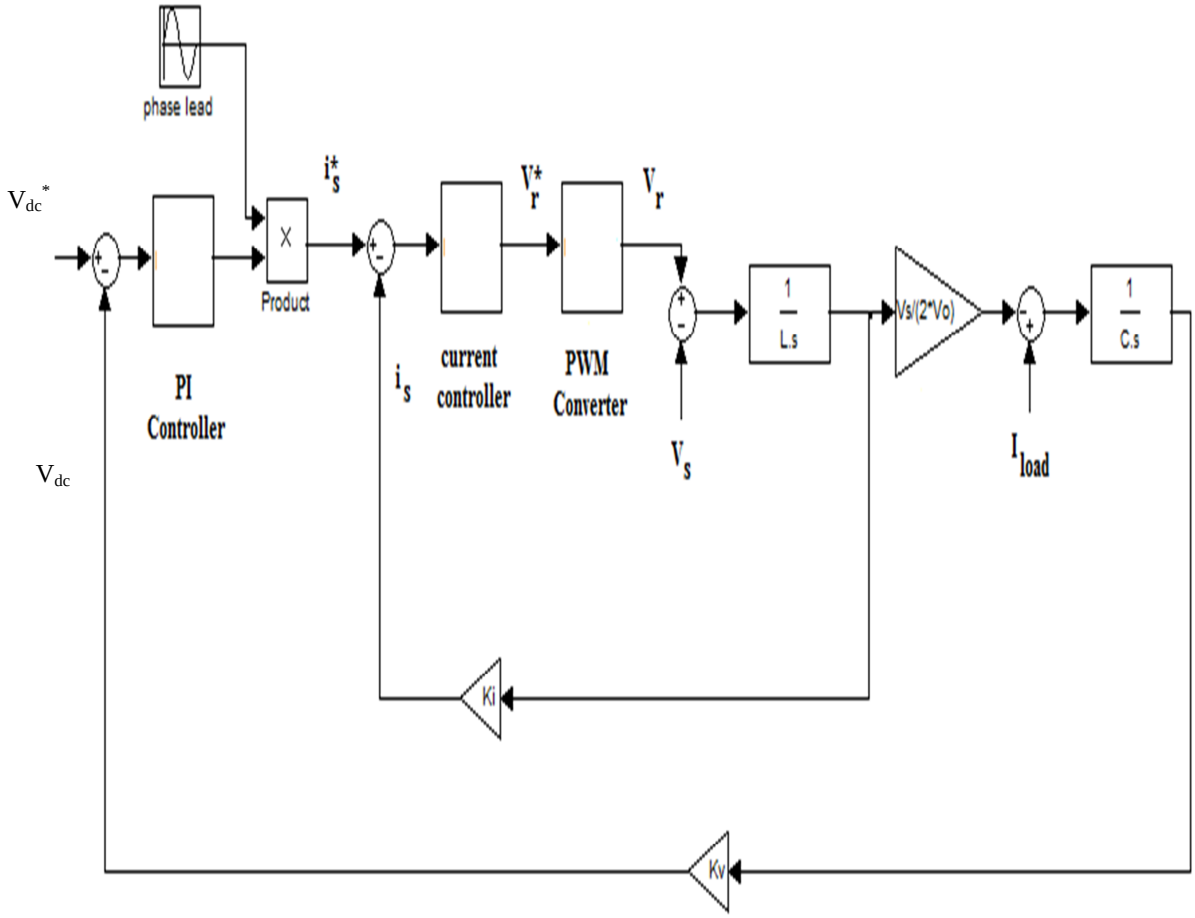

Figure 3.3 Block Diagram of Unity Power Factor Converter Control

3.2.2 Steady State Design Considerations[33]

The single-phase front-end converter shown in Figure 3.2 consists of a full-bridge converter using IGBTs, with an ac reactor at the ac input side. The converter is operated in the PWM mode with sine-triangle modulation. The supply voltage V_S and the fundamental component of V_R at the ac terminals of the converter are two sinusoidal voltages separated by a reactor. The power flow therefore depends on the phase angle displacement between the two voltage phasors. The phasor diagrams on the ac side assuming unity power factor, that is the current in phase with the supply voltage. The voltage drop across the reactance adds in quadrature to the supply voltage to give the

input ac voltage to the bridge. The magnitude of the rectifier ac input voltage is greater in magnitude than that of the supply voltage.

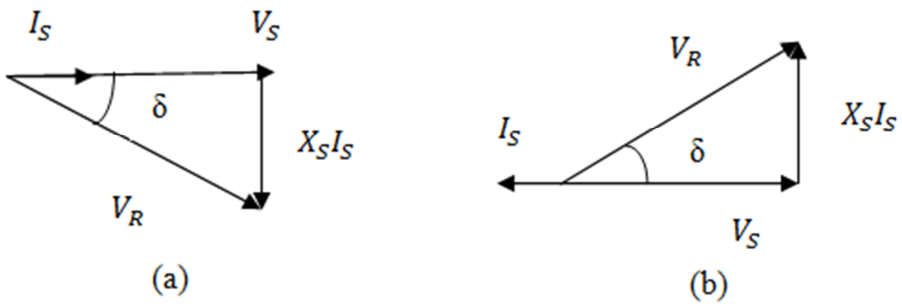

Figure. 3.4 Phasor Diagram of Front End Converter: a.)Unity Power Factor forward power flow, b.) Unity Power Factor Reverse power flow

The power flow in the inductor shown fig. 3.2 can be derived from the phasor diagram of Figure 3.4(a) or 3.4(b) as

Power = $V_s I_s$

and substituting for I_S from equation 3.2

$$V_R Sin\delta = X_S I_s \tag{3.2}$$

we get

$$Power = \frac{V_S V_R}{X_S} Sin\delta \tag{3.3}$$

Where δ is known as the displacement or load angle.

If V_R lags V_S then the power flow is from the ac supply towards the converter, but if V_R leads V_S then the power is reversed. The phasor diagrams of fig. 3.4(a) or 3.4(b) show unity power factor, but conditions involving reactive power flow, that is lagging or leading power factor are possible by changing the magnitude of one voltage while retaining the same displacement angle δ.

3.3 Dynamic Model Of Induction Motor

The steady state model of induction motor, which is represented by an equivalent circuit of induction motor, describes only steady state behaviour of the induction motor. It is used when steady state analysis, such as efficiency, losses, steady state torque, currents and fluxes are to be evaluated. Designing the machine drives based on this model will only produce a drive that normally has a poor transient performance. When machine drives for high performance application needs to be designed, a model that can describe the transient as well as the steady state behaviour of the induction machine is needed. Therefore, by using the dynamic model, the transient behaviour of the induction motor, which cannot be analysed using steady state equivalent model, can be predicted and studied.

The three phase squirrel cage induction motor in synchronous rotating reference frame can be represented as follows:

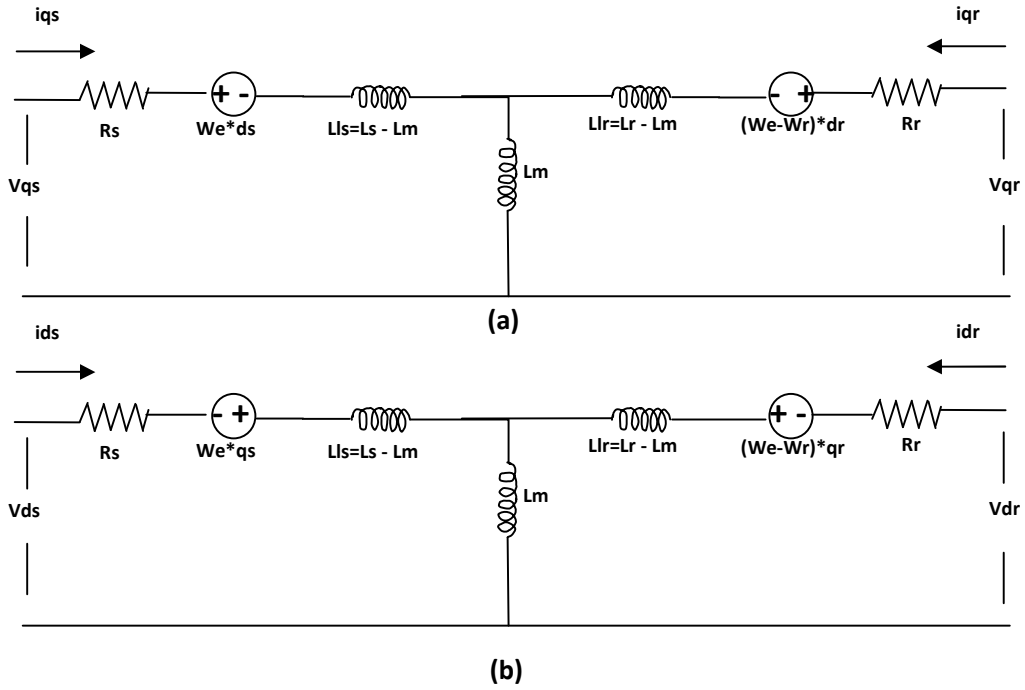

Figure 3.5 Equivalent circuit of an induction motor in the synchronous rotating reference frame, a) q-axis circuit b) d-axis circuit

The various parameters are calculated as under:

Voltage equations are

$$V_{qs} = R_s * i_{qs} + \frac{d\varphi_{qs}}{dt} + \omega_e \varphi_{ds} \tag{3.4}$$

$$V_{ds} = R_s * i_{ds} + \frac{d\varphi_{ds}}{dt} - \omega_e \varphi_{qs} \tag{3.5}$$

$$V_{qr} = R_r * i_{qr} + \frac{d\varphi_{qr}}{dt} + (\omega_e - \omega_r)\varphi_{dr} \tag{3.6}$$

$$V_{dr} = R_r * i_{dr} + \frac{d\varphi_{dr}}{dt} - (\omega_e - \omega_r)\varphi_{qr} \tag{3.7}$$

Flux equations are

$$\varphi_{qs} = L_{ls} * i_{qs} + (i_{qs} + i_{qr})L_m \tag{3.8}$$

$$\varphi_{qr} = L_{lr} * i_{qr} + (i_{qs} + i_{qr})L_m \tag{3.9}$$

$$\varphi_{ds} = L_{ls} * i_{ds} + (i_{ds} + i_{dr})L_m \tag{3.10}$$

$$\varphi_{dr} = L_{lr} * i_{dr} + (i_{ds} + i_{dr})L_m \tag{3.11}$$

Where V_{qs} & V_{ds} are the applied voltages to the stator; i_{ds}, i_{qs}, i_{dr}, & i_{qr} are the corresponding d & q axis currents; $\varphi_{qs}, \varphi_{qr}, \varphi_{ds}$ & φ_{dr} are the rotor & stator flux component; R_s, R_r are the stator & rotor resistances; L_{ls} & L_{lr} denotes the stator & rotor inductances, whereas L_m is the mutual inductance.

The electromagnetic torque equation is

$$T_e = \frac{3*P*L_m}{2*2*L_r} * (\varphi_{dr} i_{qs} - \varphi_{qr} i_{ds}) \tag{3.12}$$

Where *P* denotes the pole number of the motor

In case of vector control the *q*-component of the rotor field φ_{qr} would be zero. Then the electromagnetic torque is controlled only by *q*-axis stator current & becomes

$$T_e = \frac{3*P*L_m}{2*2*L_r} * (\varphi_{dr} i_{qs}) \tag{3.13}$$

3.4 Vector Control Methodology

Induction motor speed control methods are varied in number of ways among which vector or field oriented control is the most widely accepted methods. Vector control may be achieved using direct or indirect methods. In vector control, the same performance characteristics are obtainable as is the case with a dc motor. This is achieved by decoupling the three-phase winding into two windings (90^0 apart) so as to facilitate independent control of torque and flux.

The indirect vector control method is essentially same as the direct vector control except the unit vector generated in an indirect manner using the measured speed ω_r and slip speed ω_{sl}. The following dynamic equations take into consideration to implement indirect vector control strategy. Equation 3.14 shows the rotor flux position.

$$\theta_e = \int \omega_e dt = \int (\omega_r + \omega_{sl}) dt = \theta_r + \theta_{sl} \tag{3.14}$$

The stator current i_A, i_B, i_C in the 3-phase coordinate is changed to 2-phase AC current in the static coordinate with 3/2 equivalent transformation. Then through synchronous rotating coordinate transformation, the 2-phase AC current will be equivalent as dc current i_d and i_q in the synchronous rotating coordinate. The main features of the developed control scheme is that it uses feedforward control of the motor voltages in combination with feedback current control.

3.4.1 Control Algorithm

The currents and frequency are defined by assuming that the direct axis corresponds exactly to the angle of the rotor flux (i.e. the q axis component of the rotor flux is zero at all times). This means that the following conditions apply. Equation 3.15 shows the calculation of quadrature axis stator current, equation 3.16 shows the direct axis stator current, equation 3.17 shows the rotor flux position, equation .

$$i_{qs}^{*} = \frac{2}{3} * \frac{2}{P} * \frac{T_e * L_r}{L_m * \varphi_{dr}} \tag{3.15}$$

$$i_{ds}^{*} = \frac{\varphi_{dr}}{L_m} \tag{3.16}$$

$$\theta_e = \int \omega_e dt = \int (\omega_r + \omega_{sl}) dt = \theta_r + \theta_{sl} \tag{3.17}$$

$$\omega_r = \frac{L_m * i_{qs}}{T_e * \varphi_{dr}} \tag{3.18}$$

3.4.2 abc-dq Transformation

The *abc-dq* transformation is an essential part of this scheme. The direct–quadrature–zero (*dq*o) transformation or zero–direct–quadrature (o*dq*) transformation is a mathematical transformation used to simplify the analysis of three-phase circuits.

The transformation of abc-dq involves the decoupling of variables with time-varying coefficients and refer all variables to a common reference frame. This transformation reduces the three line currents to two dc quantities in dq reference frame. The two dc quantities are orthogonal to each other. This allows the control of the two quantities independently.

The three-phase transformation into two-phase is carried out through *abc-dq* transformation by using various methods like Stanley's transformation, Park's transformation etc. Park's transformation applied to three-phase currents is shown below in matrix form:

$$I_{dqo} = TI_{abc} = \frac{2}{3} \begin{bmatrix} \cos\theta & \cos\left(\theta - \frac{2\pi}{3}\right) & \cos\left(\theta + \frac{2\pi}{3}\right) \\ -\sin\theta & -\sin\left(\theta - \frac{2\pi}{3}\right) & -\sin\left(\theta + \frac{2\pi}{3}\right) \\ 0.5 & 0.5 & 0.5 \end{bmatrix} \begin{bmatrix} I_a \\ I_b \\ I_c \end{bmatrix} \tag{3.19}$$

The inverse transform is:

$$I_{abc} = T^{-1} I_{dqo} = \begin{bmatrix} \cos\theta & -\sin\theta & 1 \\ \cos\left(\theta - \frac{2\pi}{3}\right) & -\sin\left(\theta - \frac{2\pi}{3}\right) & 1 \\ \cos\left(\theta + \frac{2\pi}{3}\right) & -\sin\left(\theta + \frac{2\pi}{3}\right) & 1 \end{bmatrix} \begin{bmatrix} I_d \\ I_q \\ I_o \end{bmatrix} \quad (3.20)$$

3.5 Hysteresis Current Algorithm

In this circuit three phase load i.e induction motor in our case is connected to the PWM voltage source inverter. Hysteresis current algorithm is used to speed control of induction motor. The load currents i_a, i_b and i_c are compared with the reference currents i_a*, i_b* and i_c* and error signals are passed through hysteresis band to generate the firing pulses, which are operated to produce output voltage in manner to reduce the current error.

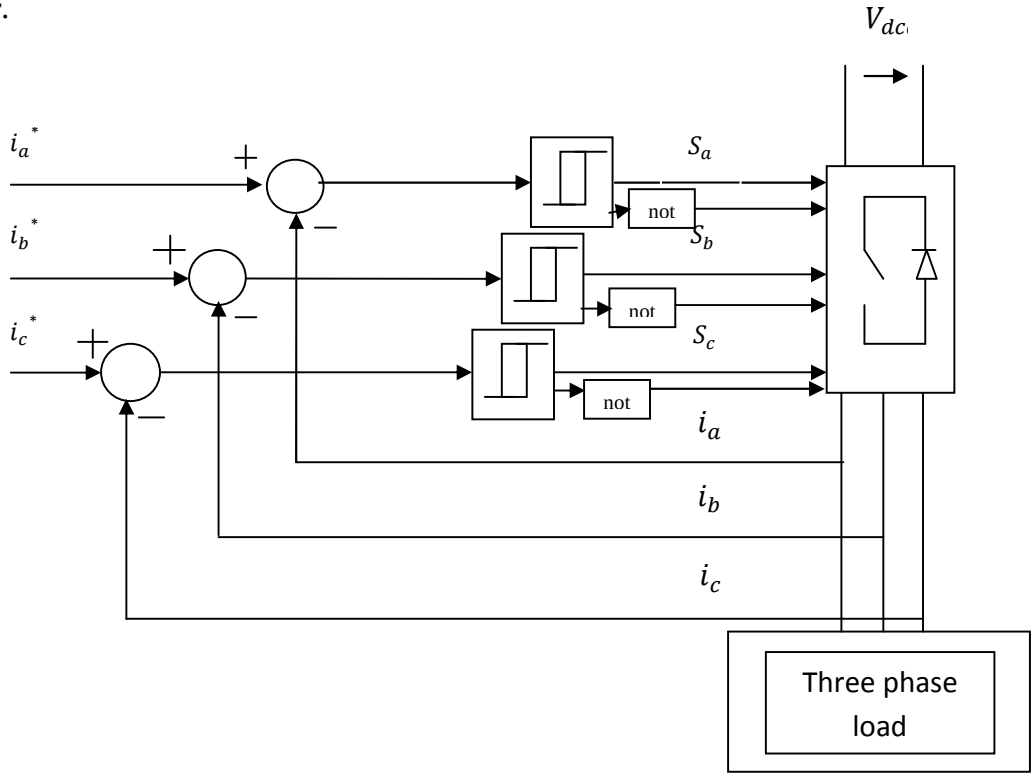

Figure 3.6 Block diagram of current hysteresis controller

The principle of Hysteresis current control is very simple. The purpose of the current controller is to control the load current by forcing it to follow a reference one. It is achieved by the switching action of the inverter to keep the current within the Hysteresis band. The load currents are sensed & compared with respective command currents by

three independent Hysteresis comparators having a hysteresis band '*h*'. The output signals of the comparators are used to activate the inverter power switches. The inverter current vector is defined as in equation 3.21

$$i = \frac{2}{3}[i_a + ai_b + a^2 i_c] \tag{3.21}$$

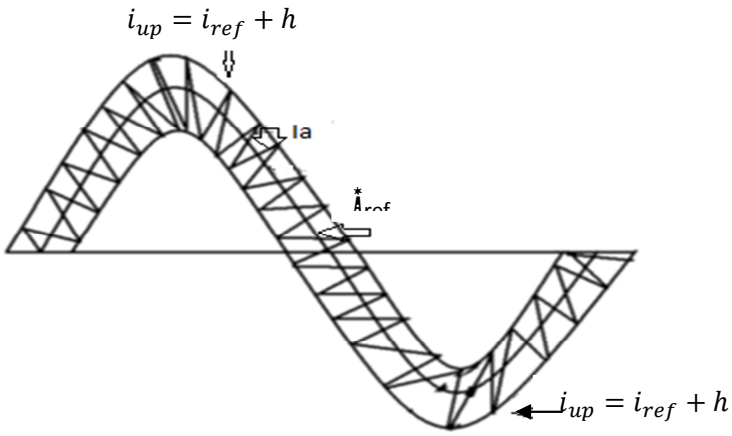

Fig.3.7 Fixed band shape of hysteresis controller

In this scheme, the hysteresis bands are fixed throughout the fundamental period. The algorithm for this scheme is given as

$$i_{ref} = i_{max} sin\omega t \tag{3.22}$$

Upper band

$$i_{up} = i_{ref} + h \tag{3.23}$$

Lower band

$$i_{low} = i_{ref} - h \tag{3.24}$$

Where *h* = Hysteresis band limit

If $i_a > i_{up}$, $V_{ao} = -V_{dc}/2$ (3.25)

If $i_a < i_{low}$, $V_{ao} = +V_{dc}/2$ (3.26)

3.6 Conclusion

In this chapter, control algorithm related to unity power control using sinusoidal pulse width modulation has been developed and its steady state design consideration has been reviewed. Also the algorithm for vector control of induction motor drive using hysteresis current control has been developed.

Chapter 4

Controller Design Using Simulink

Introduction

Simulation is the imitation of the operation of a real-world process or system over time. The act of simulating something first requires that a model be developed; this model represents the key characteristics or behaviors/functions of the selected physical or abstract system or process.

4.2 Simulink Model Of Induction Motor Drive

A computer simulation is an attempt to model a real-life or hypothetical situation on a computer so that it can be studied to see how the system works. By changing variables in the simulation, predictions may be made about the behaviour of the system. It is a tool to virtually investigate the behaviour of the system. Figure 4.1 shows the various simulink model of induction motor drive containing different subblocks. These sub blocks are explained in this chapter.

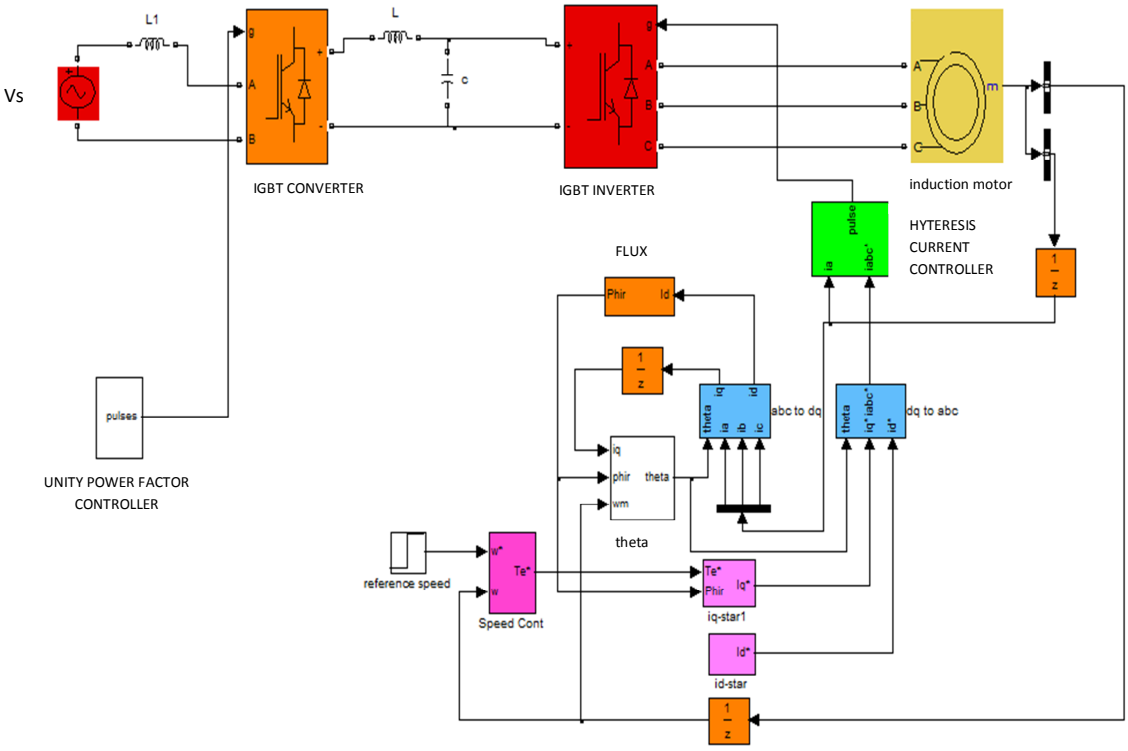

Figure 4.1 Shows the various simulink block of induction motor drive

4.2.1 Simulink Model Of Hysteresis Current Regulator

The current regulator, which consists of three hysteresis controllers, is built with Simulink blocks. The motor actual currents are provided by the measurement output of the Asynchronous Machine block. The actual motor currents and reference current are compared in hysteresis type relay.

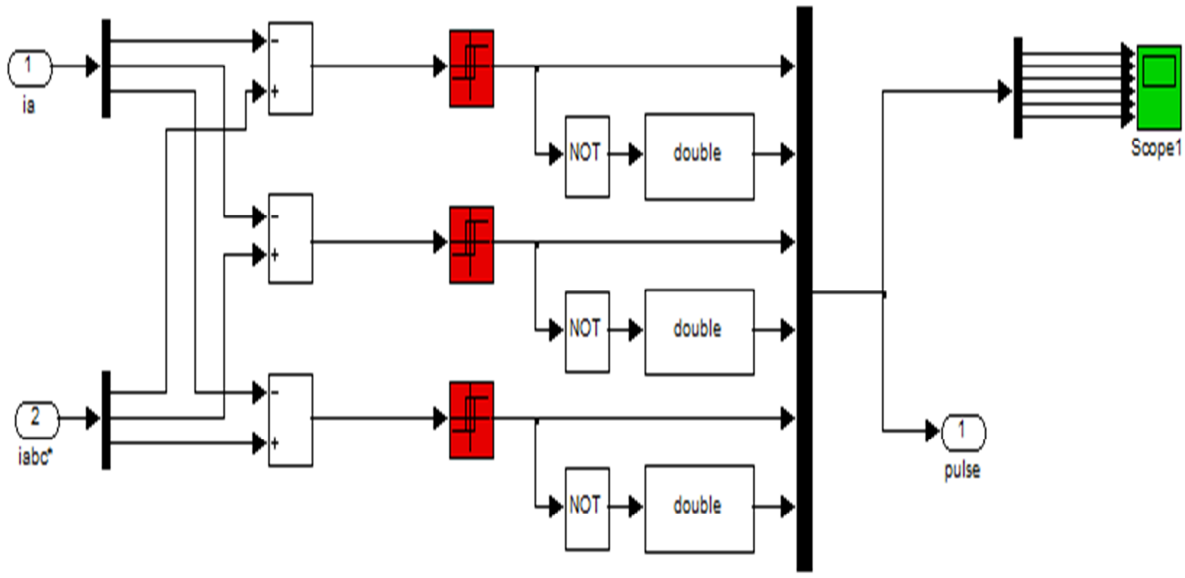

Figure 4.2 Hysteresis Current Regulator-simulink model

4.2.2 Universal Bridge:

The Universal Bridge block implements a universal three-phase power converter that consists of up to six power switches connected in a bridge configuration. The type of power switch and converter configuration is selectable from the dialog box. Power Electronic device and Port configuration options are selected as IGBT/Diode and as output terminals respectively. Set the snubber capacitance Cs to inf to get a resistive snubber.

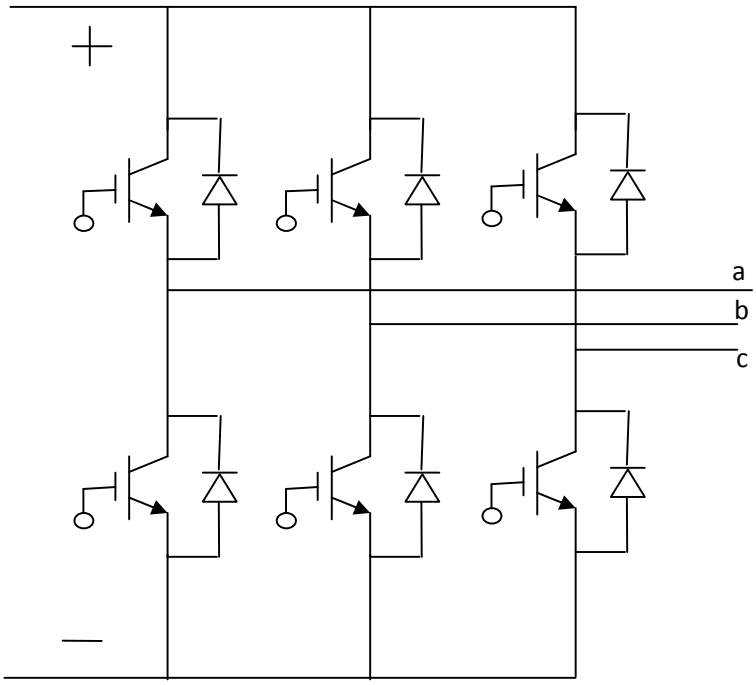

Figure 4.3 Universal Bridge block

4.2.3 Flux Calculation Simulink Model

Figure 4.4 shows the flux calculation simulink block, it is observed that flux depends on the i_d component of stator current.

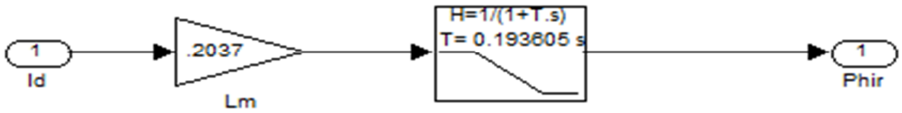

Figure 4.4 Flux Calculation Simulink Block

$$\varphi_{dr} = \frac{L_m * i_d}{1+T_r s} \quad (4.1)$$

$$L_r = Ll'_r + L_m \quad (4.2)$$

L_r= 0.005974 + 0.2037= 0.209674 H

L_m = 0.2037 H

R_r = 1.083 Ω

$$T_r = L_r / R_r = 0.19360 \text{ sec} \quad (4.3)$$

Put the value of L_m and T_r in flux equation.

4.2.4 Theta Calculation Simulink Model

Figure 4.5 shows the theta calculation simulink block. The rotor flux position (θ_e) is calculated by using equation 4.4, 4.5 and 4.6.

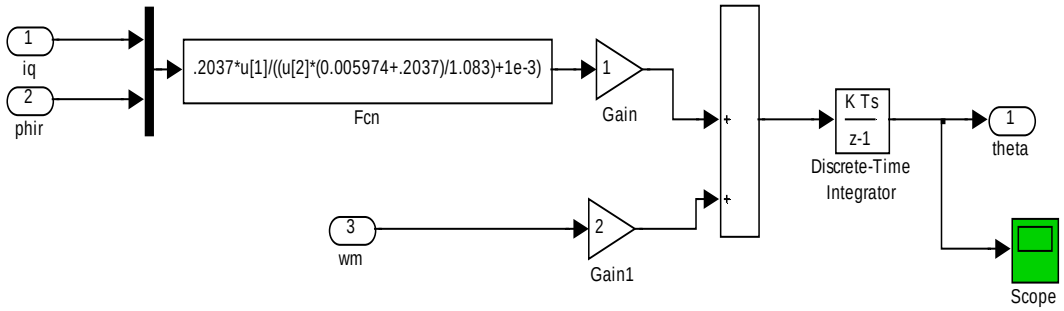

Figure 4.5 Theta Calculation Simulink block

$$\theta_e = \int \omega_e dt = \int (\omega_r + \omega_{sl}) dt = \theta_r + \theta_{sl} \tag{4.4}$$

$$\omega_r = \frac{L_m * i_{qs}}{T_e * \varphi_{dr}} \tag{4.5}$$

$$\omega_{sl} = \frac{P * \omega_m}{2} \tag{4.6}$$

4.2.5 d-q to abc Transformation Simulink Model

Figure 4.6 shows the d-q to abc transformation Simulink Block. The two-phase transformation into three-phase is carried out through *dq-abc* transformation by using Park's transformation.

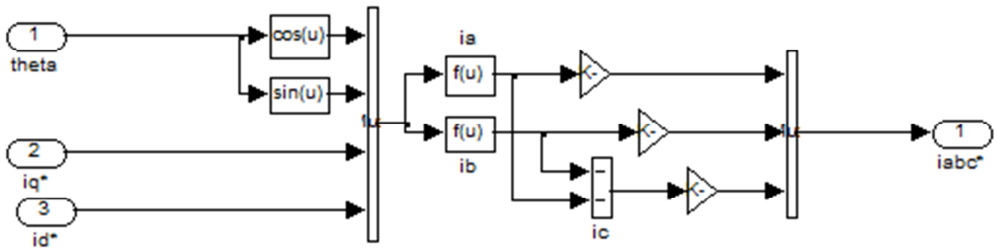

Figure 4.6 d-q to abc transformation Simulink Block

$$I_{abc} = T^{-1} I_{dqo} = \begin{bmatrix} \cos\theta & -\sin\theta & 1 \\ \cos\left(\theta - \frac{2\pi}{3}\right) & -\sin\left(\theta - \frac{2\pi}{3}\right) & 1 \\ \cos\left(\theta + \frac{2\pi}{3}\right) & -\sin\left(\theta + \frac{2\pi}{3}\right) & 1 \end{bmatrix} \begin{bmatrix} I_d \\ I_q \\ I_o \end{bmatrix} \tag{4.7}$$

4.2.6 abc to d-q Transformation Simulink Model

Figure 4.7 shows the abc to d-q Transformation Simulink Block. The three-phase transformation into two-phase is carried out through *abc-dq* transformation by using Park's transformation.

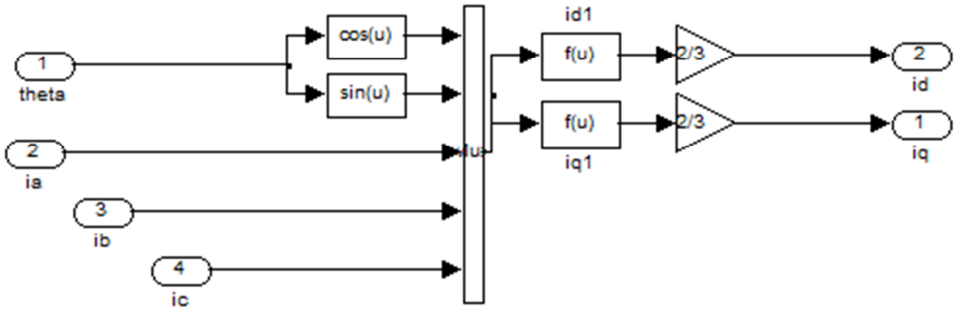

Figure 4.7 abc to d-q Transformation Simulink Block

$$I_{dqo} = TI_{abc} = \frac{2}{3}\begin{bmatrix} \cos\theta & \cos\left(\theta - \frac{2\pi}{3}\right) & \cos\left(\theta + \frac{2\pi}{3}\right) \\ -\sin\theta & -\sin\left(\theta - \frac{2\pi}{3}\right) & -\sin\left(\theta + \frac{2\pi}{3}\right) \\ 0.5 & 0.5 & 0.5 \end{bmatrix}\begin{bmatrix} I_a \\ I_b \\ I_c \end{bmatrix} \quad (4.8)$$

Here T = Transformation

4.2.7 PI Controller

Figure 4.8 shows the Proportional Integral Controller block diagram.The PI controller is used as a speed controller. The input of the PI controller is the difference between the reference speed ω* and the rotor speed ω_r. Saturation control link is used to limit the output torque.

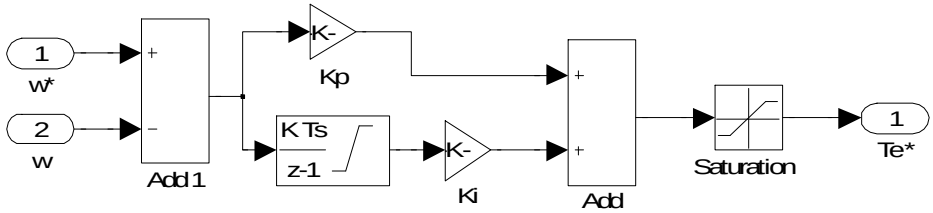

Figure 4.8 Proportional Integral Controller block diagram

The PI controller can be tuned using any method available to find out the best possible values of K_p & K_i. The tuning is done using Ziegler-Nichols method and the system is fine tuned online/manually.

4.3 Unity Power Factor Control Simulink Model

Figure 4.9 shows the Unity Power Factor Simulink Block. This block is used to switching the converter circuit in such a way that it can maintain the power factor unity at supply side.

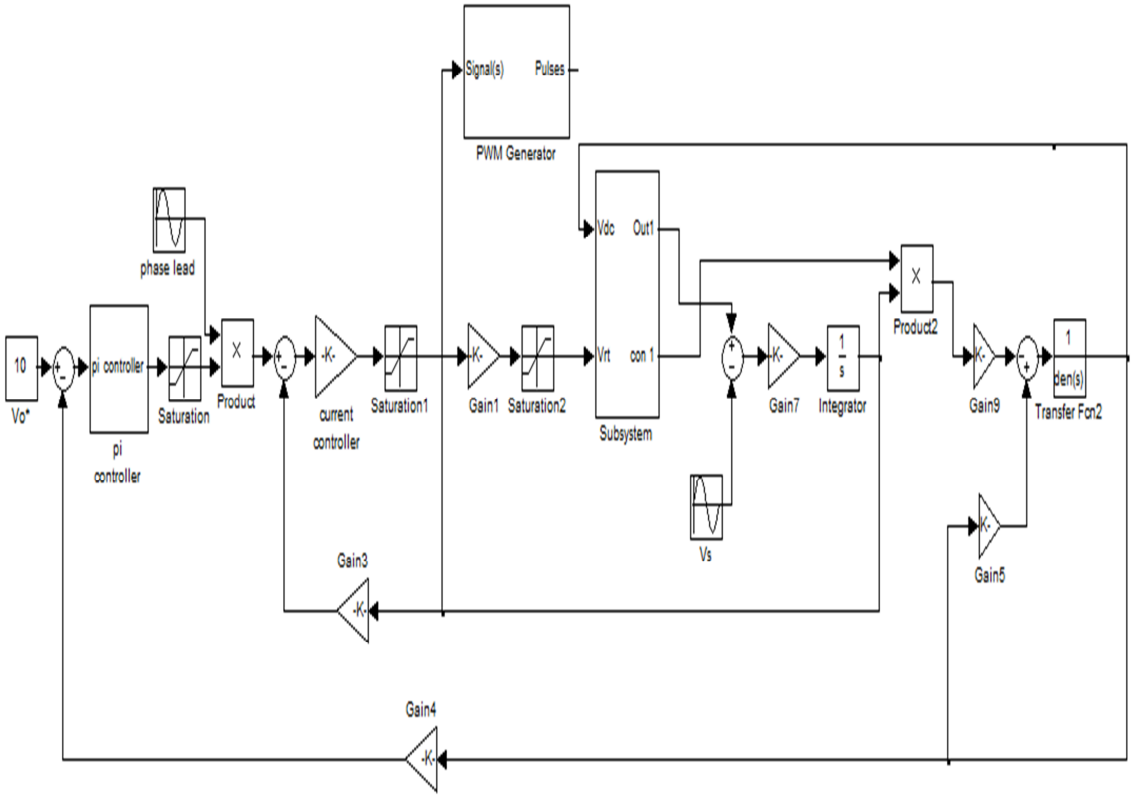

Figure 4.9 Unity Power Factor Simulink Block

4.4 Conclusion

One of the primary advantages of simulation is that they are able to provide users with feedback when designing real world systems. This allows the designer to determine the correctness and efficiency of a design before the system is actually constructed. Simulation is extensively used for educational purposes. In this chapter simulink model of induction motor drives has been presented. Different simulink block such as hysteresis current regulator, flux calculation block, theta calculation block, PI controller, unity power factor controller, abc to d-q and d-q to abc have been discussed and explained.

Chapter 5

Simulation Results

Introduction

There are two big advantages by performing a simulation studies rather than actually design and testing it. The biggest of these advantages is money. Designing, testing, redesigning, retesting for anything can be an expensive project. Most of the time the simulation testing is cheaper and faster than performing the multiple tests of the design each time.

The second biggest advantage of a simulation studies is the level of detail that you can get from a simulation. A simulation can give the results that are not experimentally measurable with the current level of technology.

5.2 Implementation In Matlab

In order to show unity power factor at supply side and indirect vector controller designed using hysteresis current algorithm, the simulation has been carried on the 3-phase, 5hp(3.73KW), 1750rpm (183.33rad/sec), 50Hz squirrel cage induction motor with following parameters:

Stationary reference frame

Y- Connected

R_s (stator resistance) = 1.115Ω

R_r (rotor resistance) = 1.083Ω

L_s (stator inductance) = 0.005974H

L_r (rotor inductance) = 0.005974H

L_m (magnetizing inductance) = 0.2037H

J (moment of inertia) = 0.02Kg m^2

P (number of poles) = 4

The simulation is carried out at different speed for both no load and full load. The MATLAB 7.7.0 (R2008b) based simulink diagram is shown for the unity power factor control for the induction motor in Figure 5.1.

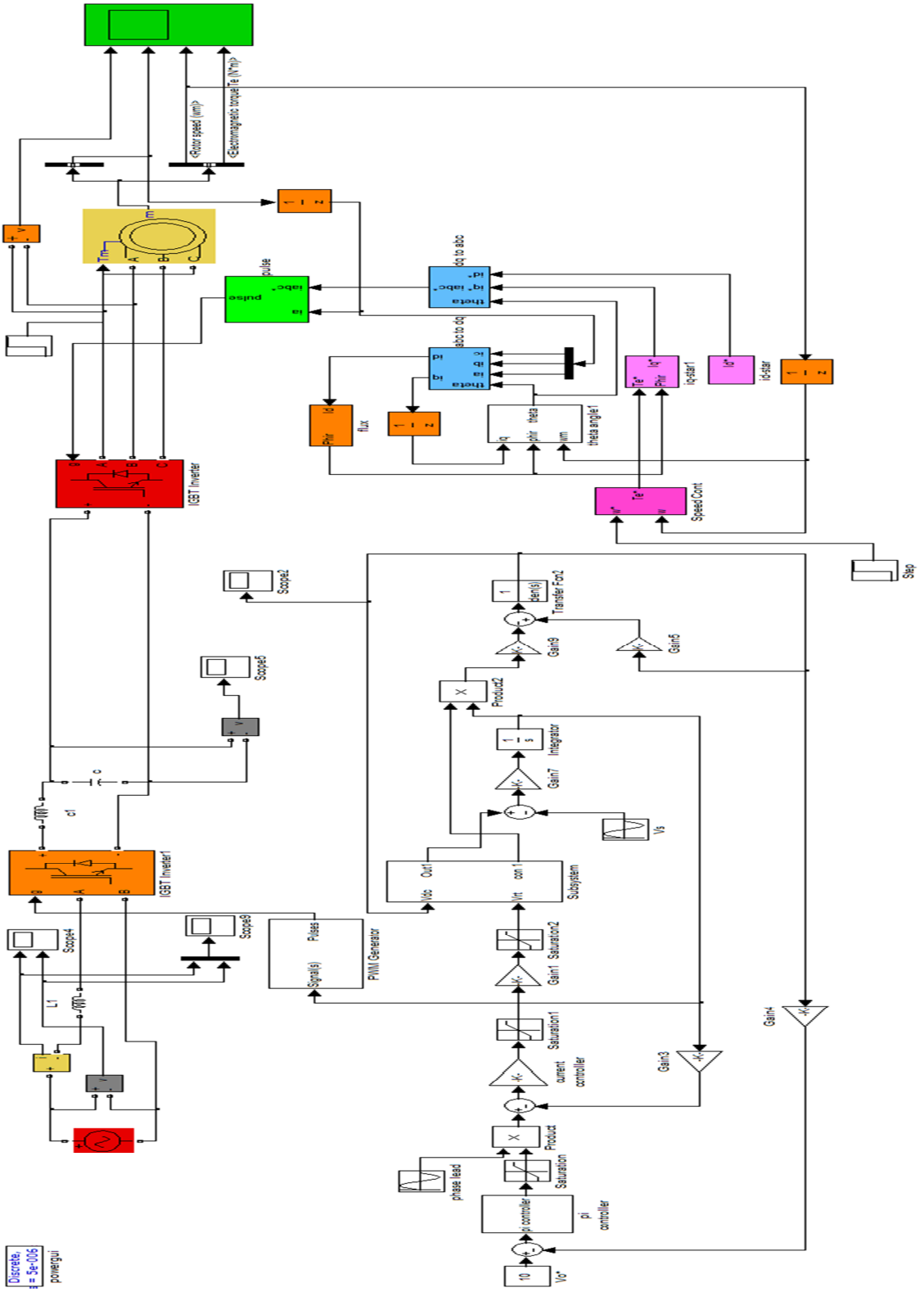

Figure 5.1 Implementation of unity power factor control of induction machine

5.3 Simulink Results

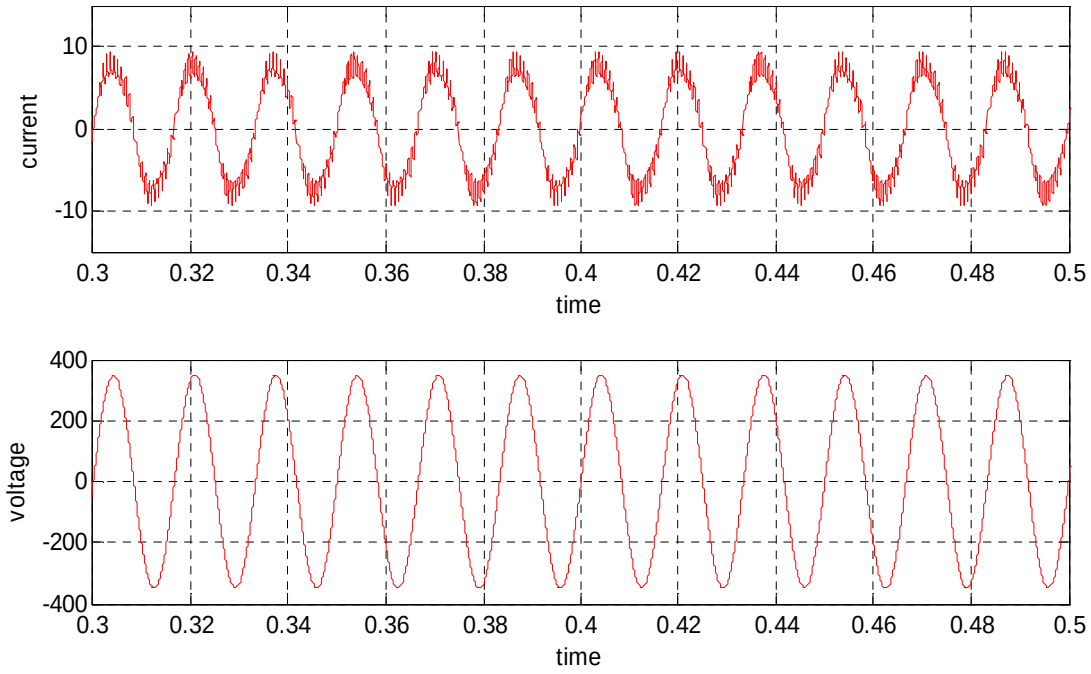

(a)

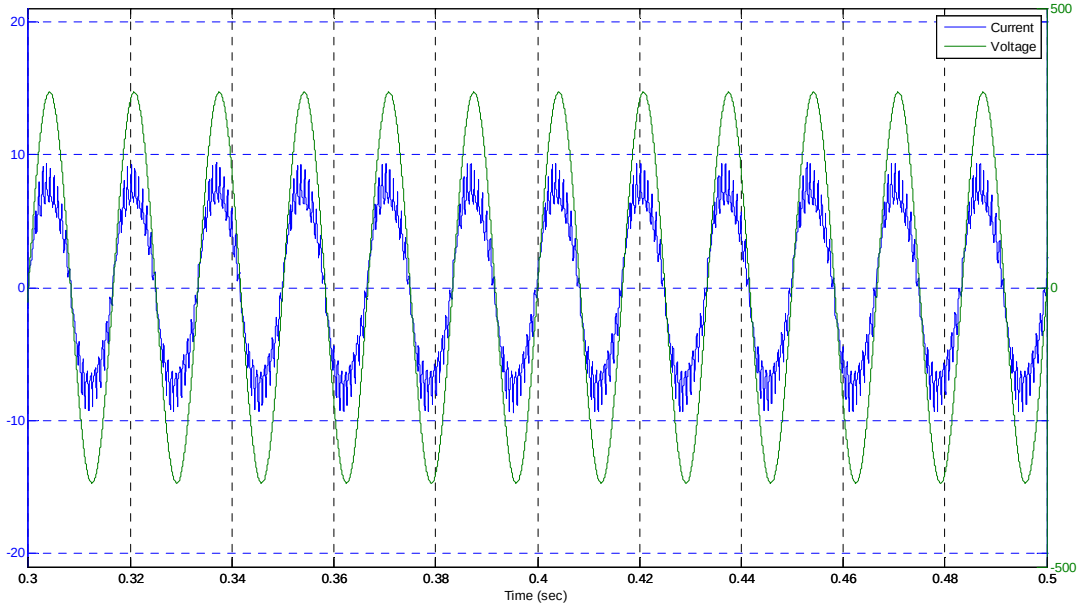

(b)

Figure 5.2(a) and 5.2(b) Simulink plot showing supply side unity power factor control on "no load" at 60 rad/sec

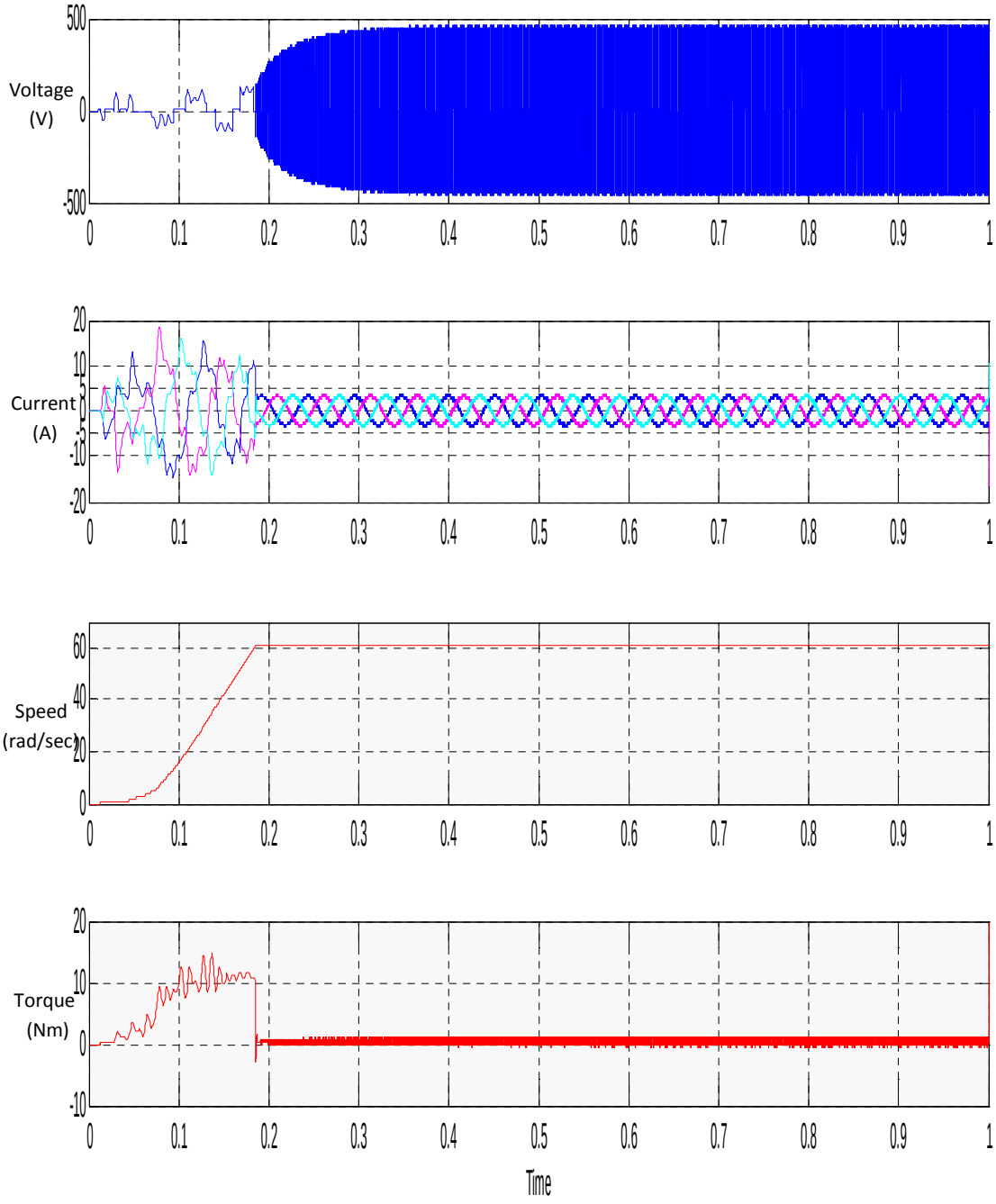

Figure 5.3 Simulink plot showing voltage(line-line), three phase stator current, speed and electromagnetic torque on "no load" at 60rad/sec speed

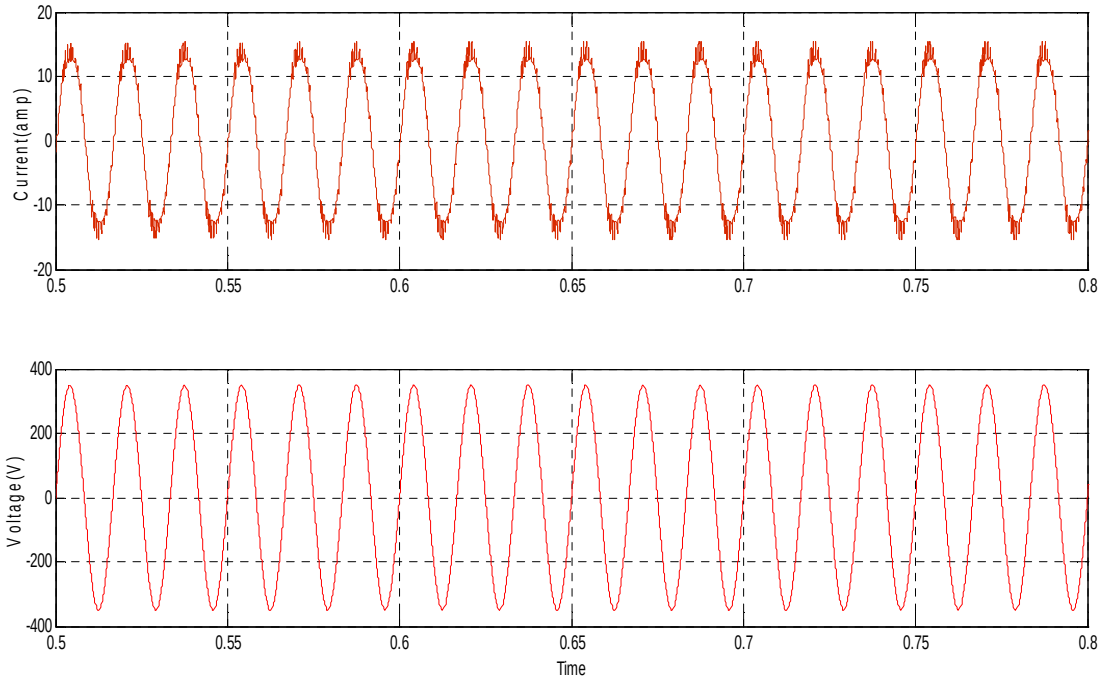

(a)

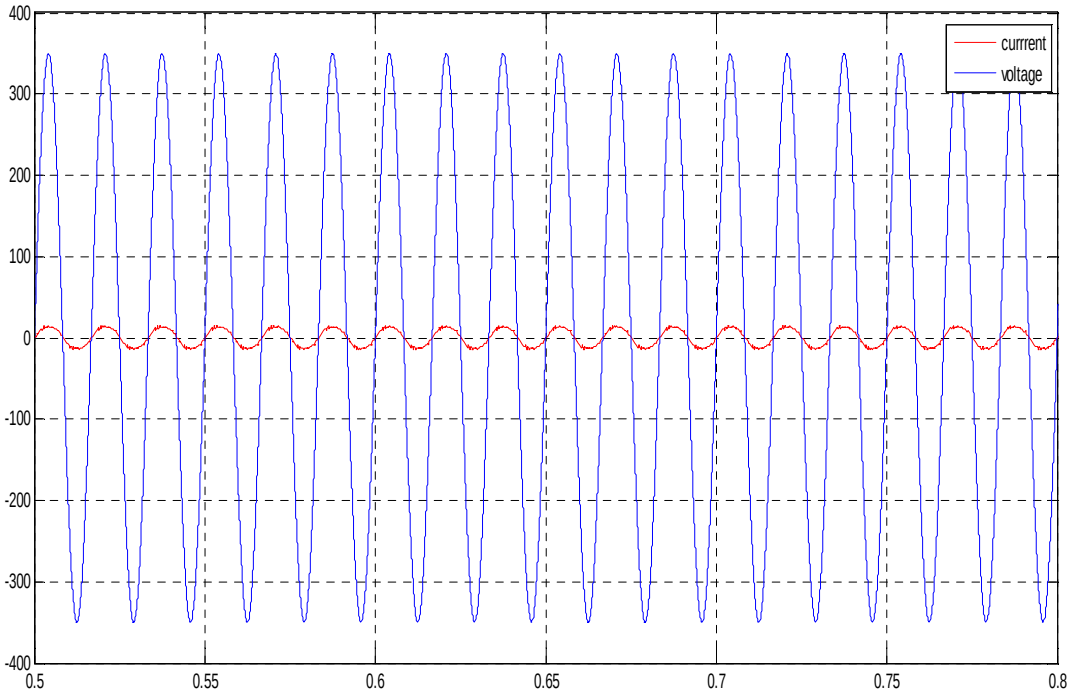

(b)

Figure 5.4(a) and 5.4(b) Simulink plot showing supply side unity power factor control on "full load" at 60 rad/sec

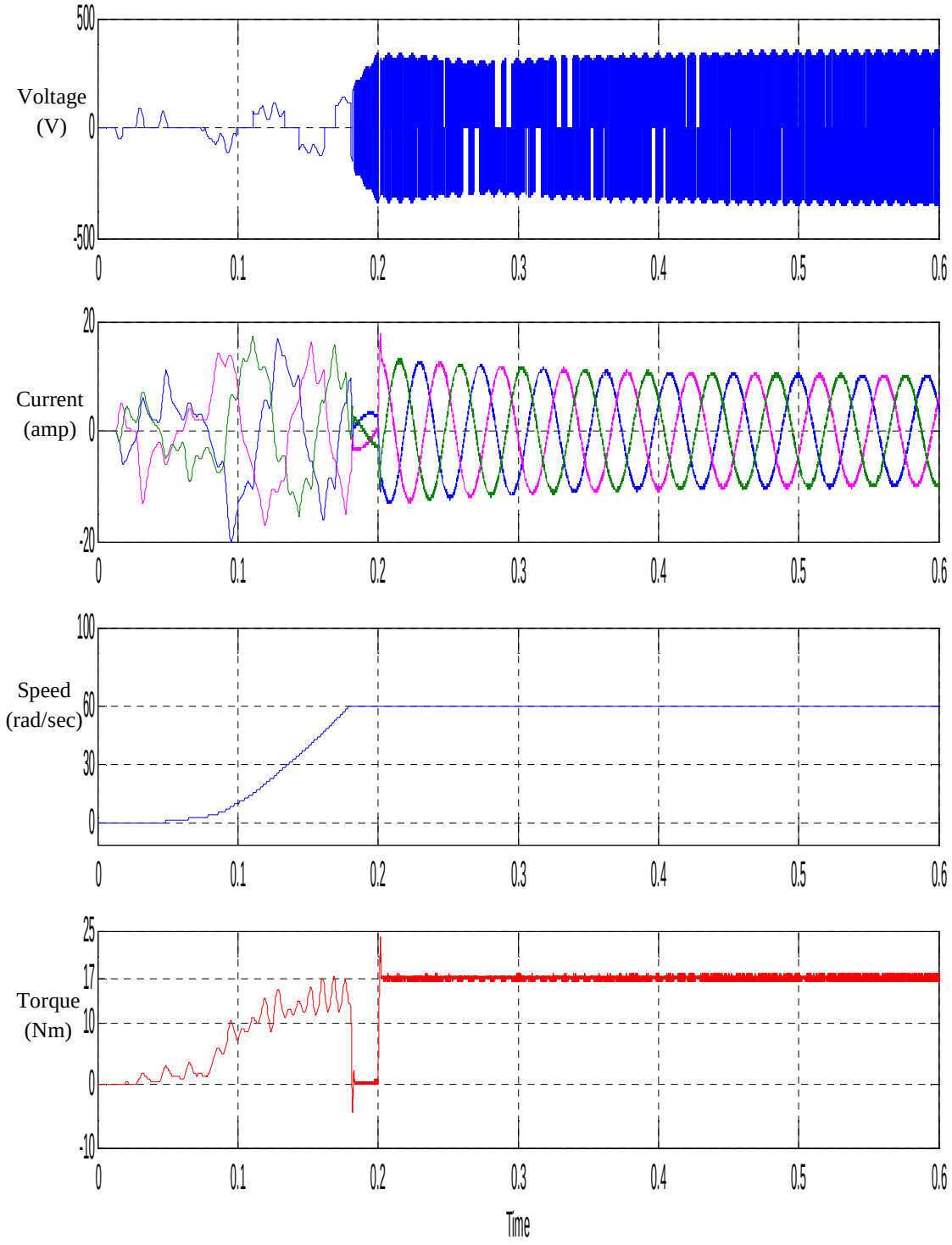

Figure 5.5 Simulink plot showing voltage(line-line), three phase stator current, speed and electromagnetic torque on "full load" at 60rad/sec speed

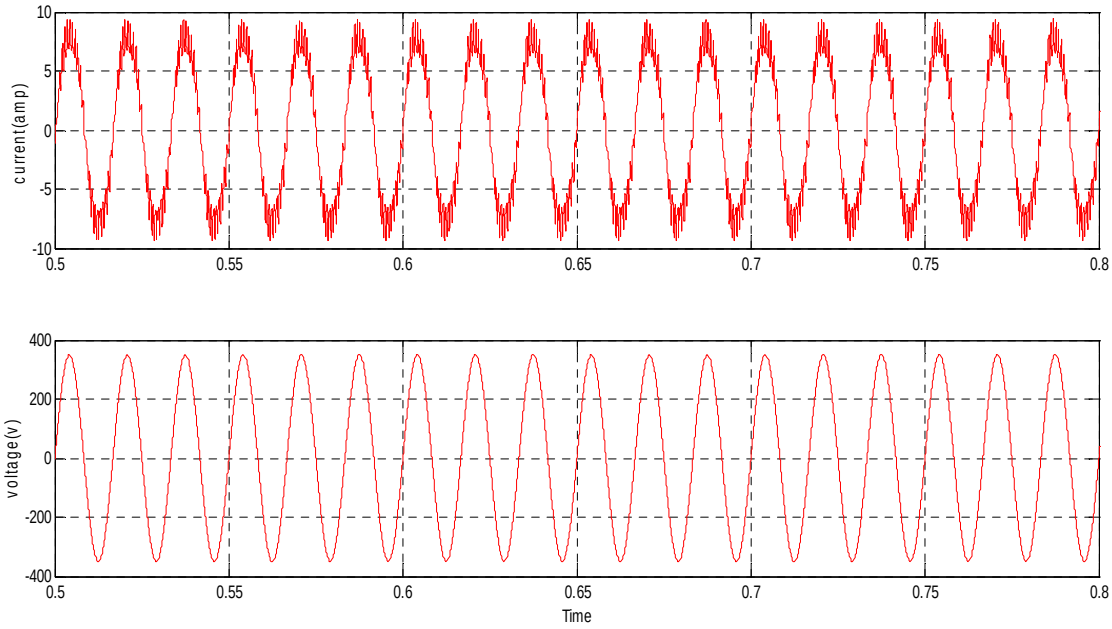

(a)

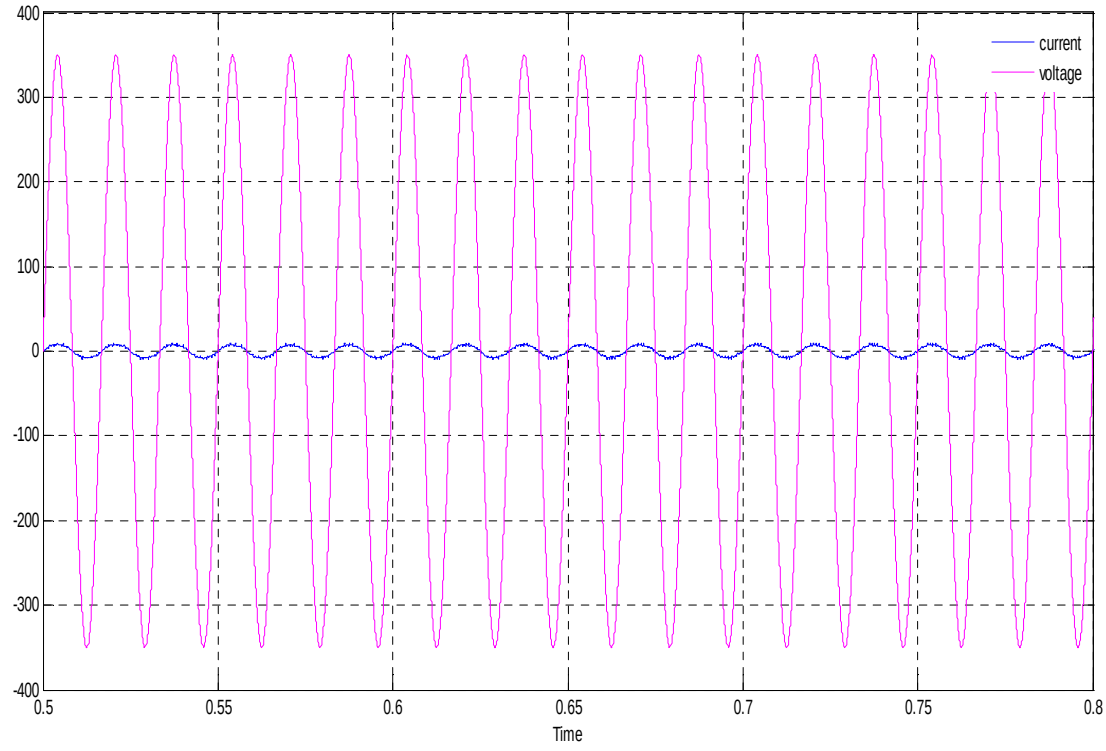

(b)

Figure 5.6(a) and 5.6(b) Simulink plot showing supply side unity power factor control on "no load" at 150 rad/sec

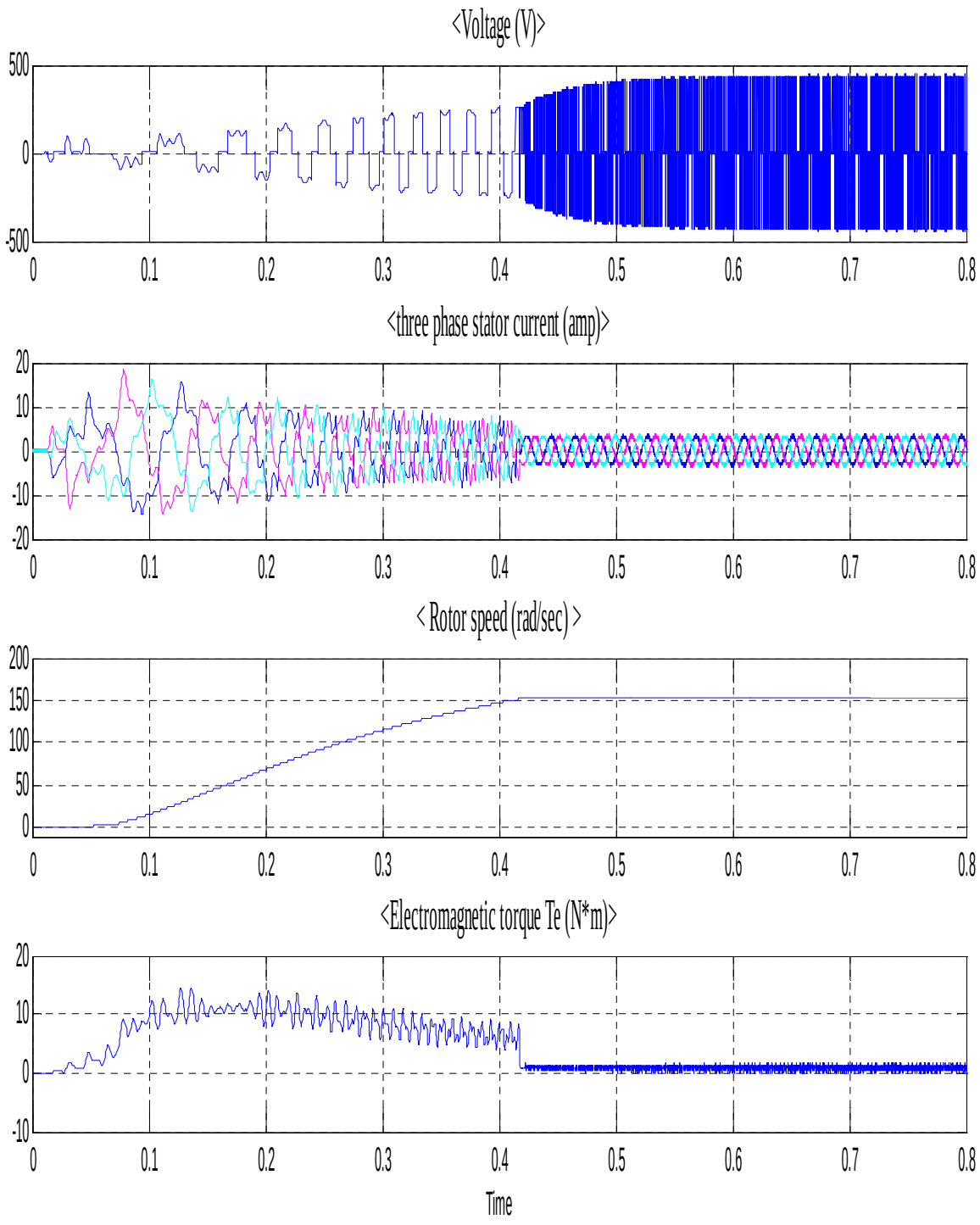

Figure 5.7 Simulink plot showing voltage(line-line), three phase stator current, speed and electromagnetic torque on "no load" at 150rad/sec speed

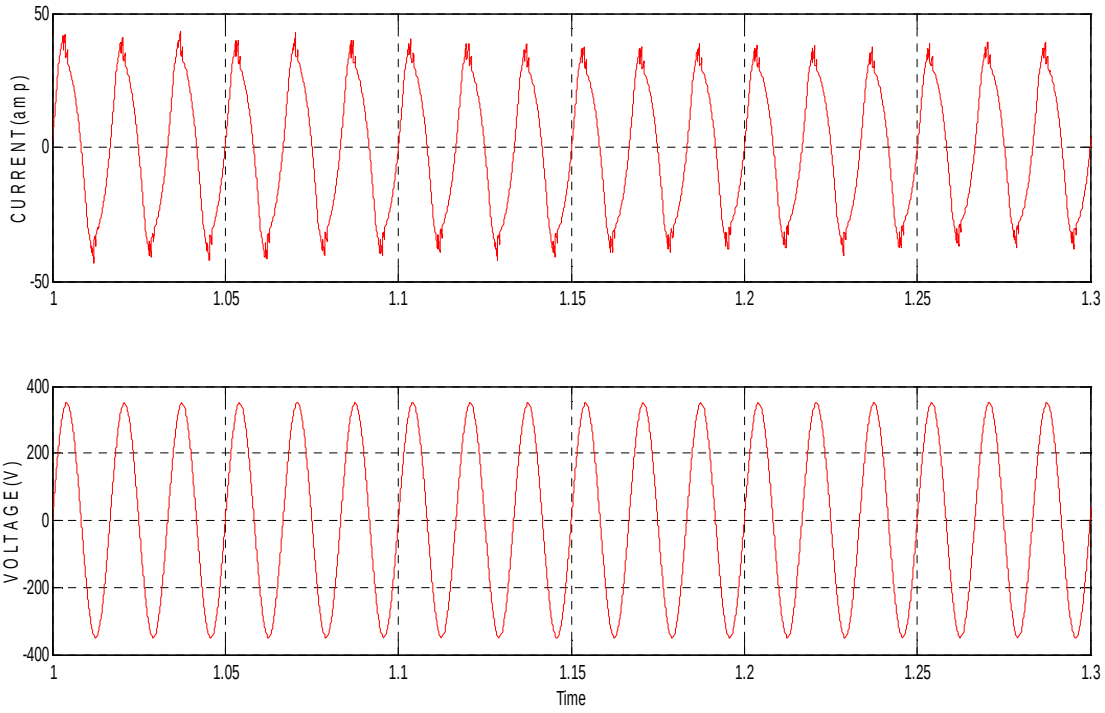

(a)

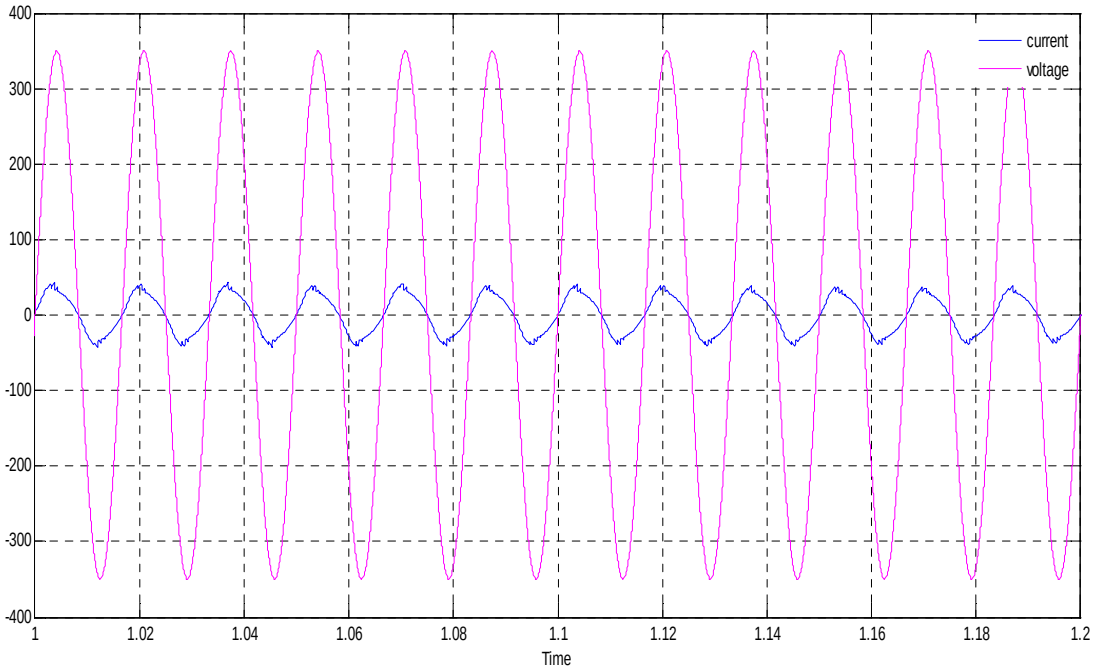

(b)

Figure 5.8(a) and 5.8(b) Simulink plot showing supply side unity power factor control on "full load" at 140 rad/sec

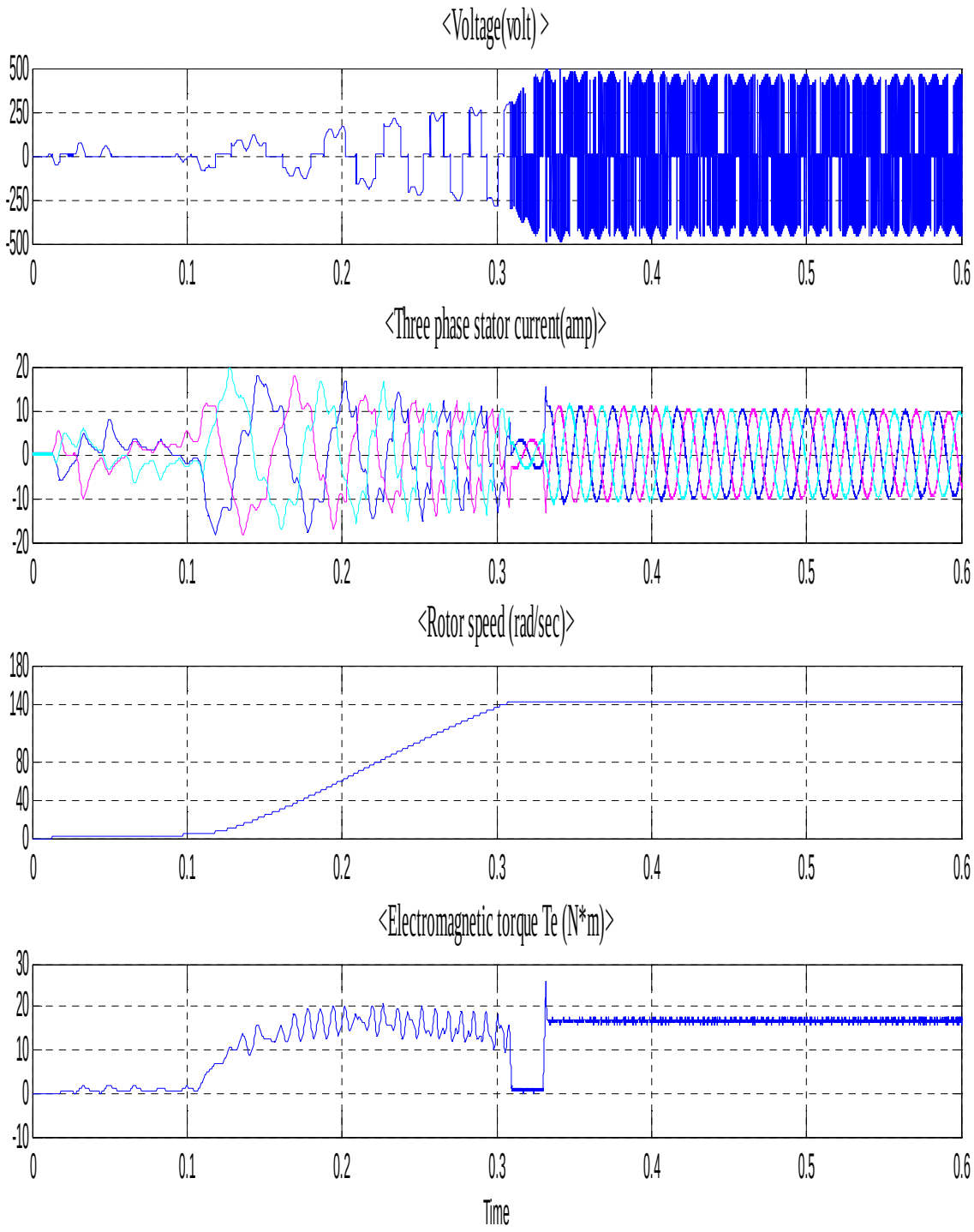

Figure 5.9 Simulink plot showing voltage(line-line), three phase stator current, speed and electromagnetic torque on "full load" at 140rad/sec speed

The simulation has also been carried on the large rating 3-phase 220KW, 1750rpm (183.33rad/sec), 50Hz rating squirrel cage induction motor with following parameters:

Stationary reference frame
Y- Connected,

R_s (stator resistance) = 0.01485Ω

R_r (rotor resistance) = 0.009295Ω

L_s (stator inductance) = 0.0003027H

L_r (rotor inductance) = 0.0003027H

L_m (magnetizing inductance) = 0.010.46H

J (moment of inertia) = 3.1Kg m^2

P (number of poles) = 4

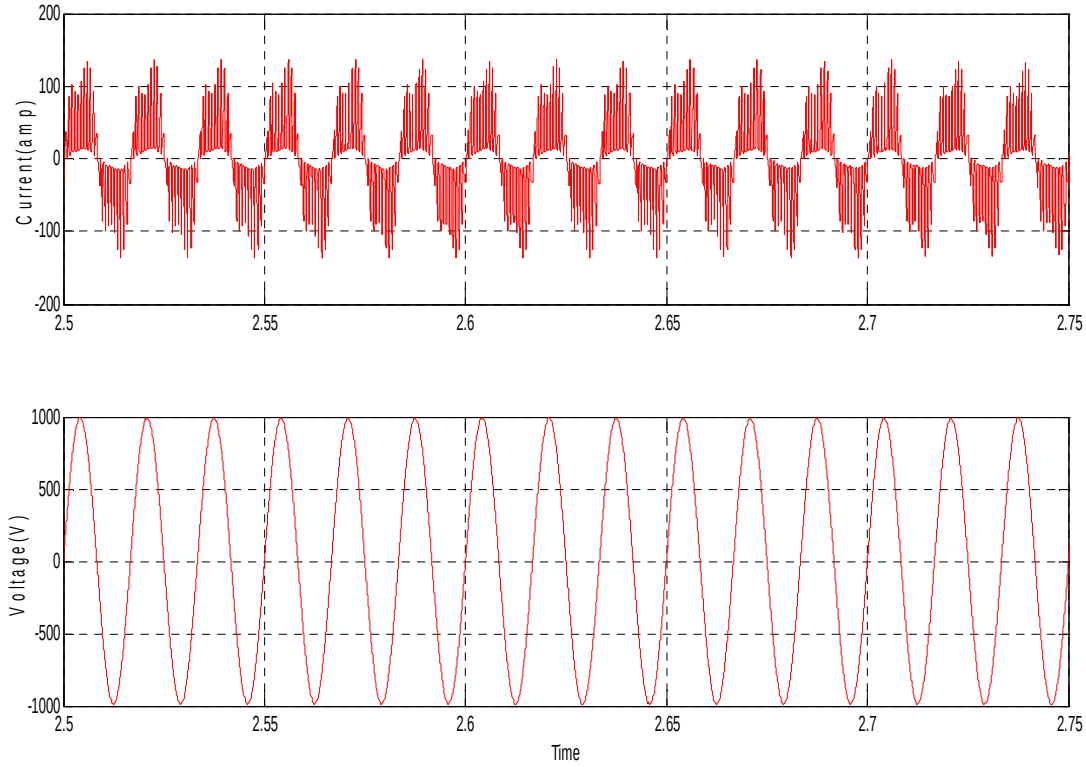

(a)

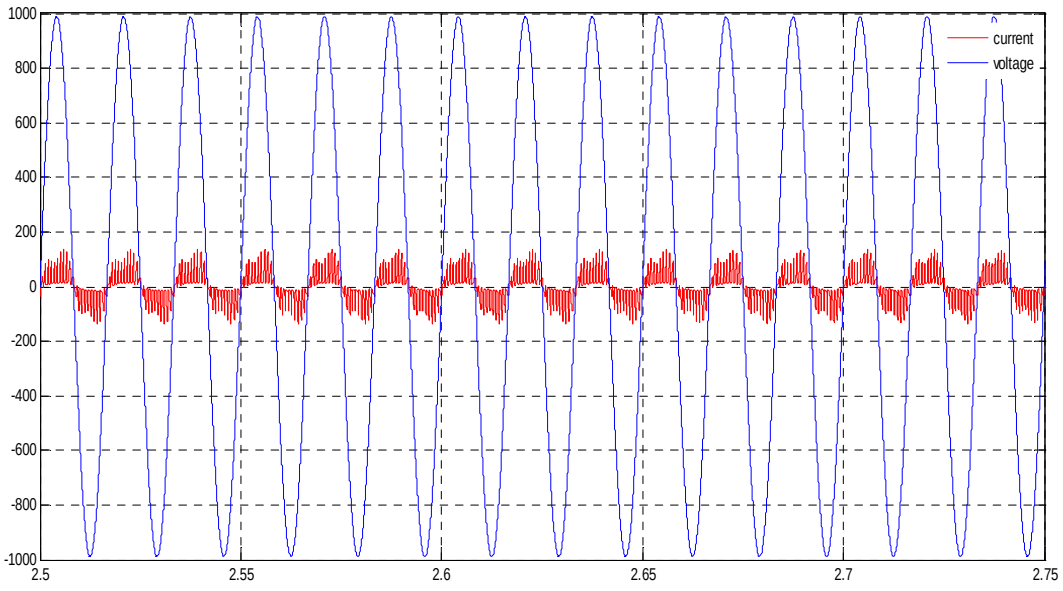

(b)

Figure 5.10(a) and 5.10(b) Simulink plot showing supply side unity power factor control on "no load" at 140 rad/sec

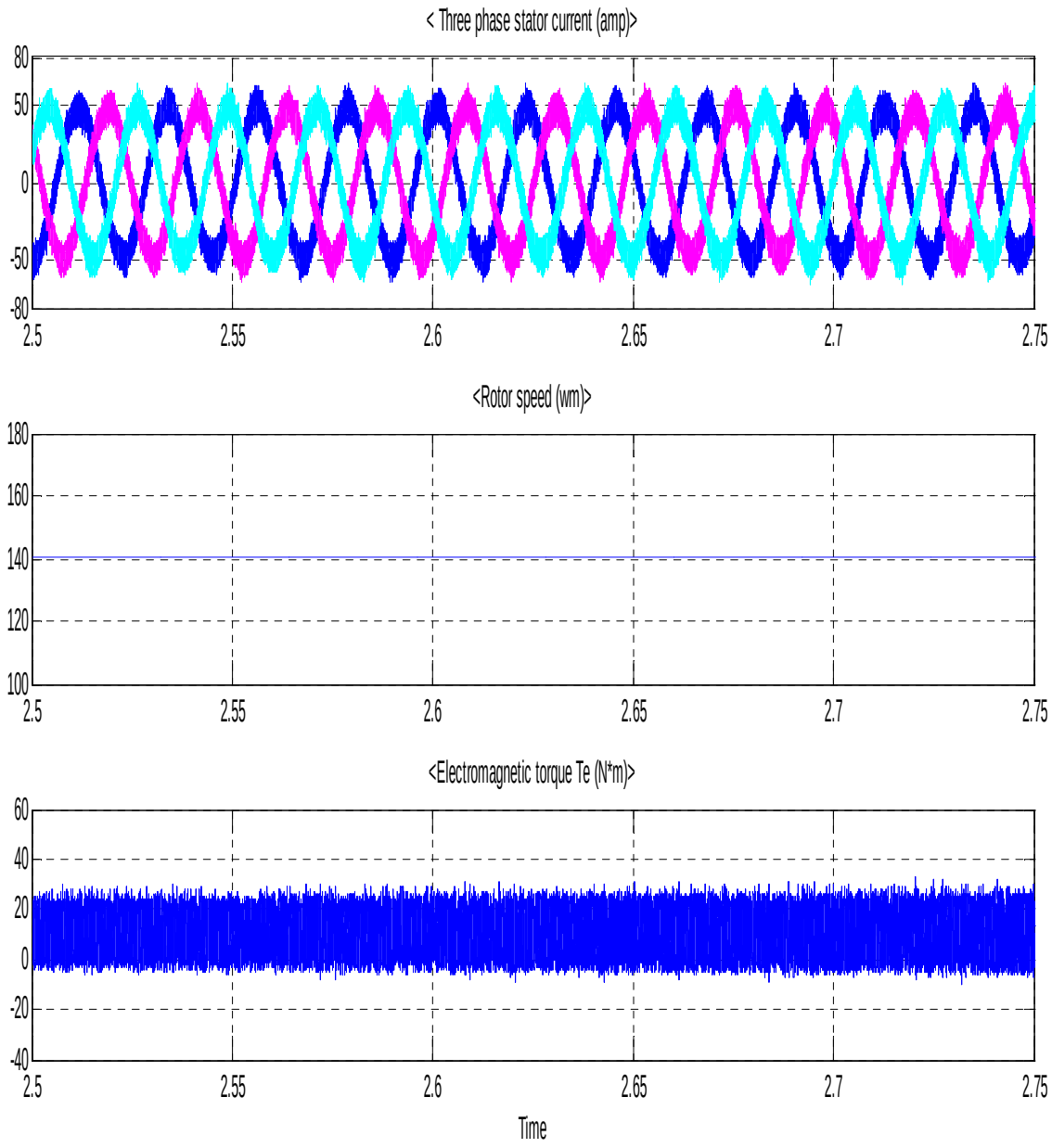

Figure 5.11 Simulink plot showing three phase stator current, speed and electromagnetic torque on no load at 140rad/sec speed

5.4 Results Analysis

Figure 5.2(a) and 5.2(b) shows the simulink results of supply side unity power factor control of 5hp induction motor working on “no load” at 60 rad/sec. It has been observed that at no load supply side current is 8.1 A peak current but at improved power factor of approximately unity. The current contains nominal harmonics.

Figure 5.3 shows voltage(line-line), three phase stator current, speed and electromagnetic torque of 5hp induction motor on “no load” at 60 rad/sec. The no load current per phase is 3.2 A peak. The currents show a hysteresis band of variation. The three phase currents are perfectly sinusoidal, 120^{o} apart from each other. At the time of starting the maximum current drawn by the induction motor is as high as 18 A peak.

Figure 5.4(a) and 5.4(b) shows the simulink results of supply side unity power factor control of 5hp induction motor working on “full load” at 60 rad/sec, it has been observed that at full load supply side current is 12.1 A peak current but at improved power factor of approximately unity. The current contains nominal harmonics.

Figure 5.5 shows voltage(line-line), three phase stator current, speed and electromagnetic torque of 5hp induction motor on “full load” at 60 rad/sec. The full load current is 9.4 A peak. The current show a hysteresis band of variation. The three phase currents are perfectly sinusoidal, 120^{o} apart from each other. At the time of starting the maximum current drawn by the induction motor is as high as 18 A peak.

Figure 5.6(a) and 5.6(b) shows the simulink results of supply side unity power factor control of the same 5hp induction motor working on “no load” at 150 rad/sec. It has been observed that at no load supply side current 8.1 A peak current but at improved power factor of approximately unity. The current contains nominal harmonics.

Figure 5.7 shows voltage(line-line), three phase stator current, speed and electromagnetic torque of 5hp induction motor on “no load” at 150 rad/sec. The no load current is 3.2 A peak. The currents show a hysteresis band of variation. The three phase

currents are perfectly sinusoidal, 120^o apart from each other. At the time of starting the maximum current drawn by the induction motor is as high as 18 A peak

Figure 5.8(a) and 5.8(b) shows the simulink results of supply side unity power factor control of 5hp induction motor working on "full load" at 140 rad/sec, it has been observed that at full load supply side current is 30 A peak current but at improved power factor of approximately unity, the current contains harmonics.

Figure 5.9 shows voltage(line-line), three phase stator current, speed and electromagnetic torque of 5hp induction motor on "full load" at 140 rad/sec. The full load current per phase is 9.4 A peak. The current show a hysteresis band of variation. The three phase currents are perfectly sinusoidal, 120^o apart from each other. At the time of starting the maximum current drawn by the induction motor is as high as 18 A peak.

Figure 5.10(a) and 5.10(b) shows the simulink results of supply side unity power factor control of 220KW induction motor working at no load. It has been observed that with the present scheme at no load the power factor approaches unity. As compared to low rating motor , the current drawn by 220KW induction motor contains a substantial harmonics which can be minimized using active filters.

Figure 5.11 shows the simulink result of three phase stator current, speed and electromagnetic torque on no load at 140 rad/sec speed. The no load current is 50 A peak. The current is using hysteresis controller so a current profile will show a hysteresis band of variation. The three phase currents are perfectly sinusoidal, 120^o apart from each other.

5.5 Conclusion

In the chapter simulink results of power factor control of induction motor drive working at no load and full load are presented. The results are taken for different values of speeds.In order to optimum utilize the model, the simulation studies of large rating motor for power factor control is also done and results are presented.

Chapter 6

Conclusion and Further Scope

6.1 Conclusion

Now a days induction motor drive has became a standard in transportation industry and for agriculture functions, it is therefore desired that these motor shall work efficiently, maintaining the unity power factor of utility supply system and draw minimum reactive power from the sources.

In the report, an extensive review of power factor control of induction motor drive is presented. Algorithm related to unity power control using sinusoidal pulse width modulation has been developed and its steady state design consideration has been reviewed. Also the algorithm for vector control of induction motor drive using hysteresis current control has been developed. This algorithm has been applied to develop simulink model of induction motor drives using different simulink block such as hysteresis current regulator, flux calculation block, theta calculation block, PI controller, unity power factor controller, abc to d-q and d-q to abc. These block have been discussed and explained in the report.

Using the developed simulink model, simulation studies have been carried out to control the speed of induction motor and enhancing the power factor control to unity. The speed is controlled using hysteresis current controller, which controls the frequency of stator current. The results are taken for different values of speed, it has been observed that the power factor can be controlled to unity at both the speeds. The simulation studies are done under both no load and full load condition. In order to optimum utilization of the model, the simulation studies are carried out for different rating induction motor, power factor control is also done and results are presented.

6.2 Further Scope

A number of control techniques are available today that can be implemented to improve the performance of the drive.We already have the conventional PID technique to improve the performance of the PI controller. The PI & FLC can be implemented in coordination to obtain a better performance. Besides this, also focusing on the hysteresis

current control techniques, we have the SVPWM technique to obtain better control in the circuit. A synchronous current control voltage PWM can also be used.

Speed Sensorless vector control is an emerging technology. A number of speed estimation techniques are being reviewed. However, very low-speed operation including start-up at zero frequency remains a challenge. Besides Sensorless Vector Control Scheme, Direct Torque Control Scheme can also be used. Its response has been found to be more superior to FOC scheme. High efficiency & low losses - switching losses are minimized because the transistors are switched only when it is needed to keep torque and flux within their hysteresis bands.

Harmonics in the supply current can be reduced further by using the active power filter and also by using multilevel converter.

References

[1] K. Thiyagarajah, V. T. Ranganathan and B. S. Ramakrishna Iyengar, "A High Switching Frequency IGBT PWM Rectified Inverter System for AC Motor Drives Operating from Single Phase Supply", *IEEE Transactions On Power Electronics.* vol. 6, no. 4. october 1991.

[2] Adrian David Cheok, Shoichi Kawamoto, Takeo Matsumoto, and Hideo Obi , "High Power AC/DC Converter and DC/AC Inverter for High Speed Train Applications", 0-7803-6355-8/00/$10.00@ IEEE, 2000.

[3] P. Enjeti and A. Rahman, "A new single phase to three phase converter with active input current shaping for low cost AC motor drives", *IEEE Trans. Ind. Appl.*, vol. 29, no. 2, pp. 806–813, Jul./Aug. 1993.

[4] J. Itoh and K. Fujita, "Novel unity power factor circuits using zero-vector control for single-phase input systems", *IEEE Trans. Power Electron.*, vol. 15, no. 1, pp. 36–43, Jan. 2000.

[5] B. K. Lee, B. Fahimi, and M. Ehsani, "Overview of reduced parts converter topologies for AC motor drives", in *Proc. IEEE PESC*, 2001, pp. 2019–2024.

[6] C. B. Jacobina, M. B. de R. Correa, A. M. N. Lima, and E. R. C. da Silva, "AC motor drive systems with a reduced switch count converter", *IEEE Trans. Ind. Appl.*, vol. 39, no. 5, pp. 1333–1342, Sep./Oct. 2003.

[7] R. Q. Machado, S. Buso, and J. A. Pomilio, "A line-interactive single- phase to three-phase converter system", *IEEE Trans. Power Electron.*, vol. 21, no. 6, pp. 1628–1636, May 2006.

[8] O. Ojo, W. Zhiqiao, G. Dong, and S. Asuri, “High-performance speed- sensorless control of an induction motor drive using a minimalist single- phase PWM converter”, *IEEE Trans. Ind. Appl.*, vol. 41, no. 4, pp. 996– 1004, Jul./Aug. 2005.

[9] J. R. Rodrıguez, J. W. Dixon, J. R. Espinoza, J. Pontt, and P. Lezana, “PWM regenerative rectifiers: State of the art”, *IEEE Trans. Ind. Electron.*, vol. 52, no. 1, pp. 5–22, Feb. 2005.

[10] D.C. Lee and Y.S. Kim, “Control of single-phase-to-three-phase AC/DC/AC PWM converters for induction motor drives”, *IEEE Trans. Ind. Electron.*, vol. 54, no. 2, pp. 797–804, Apr. 2007.

[11] F. Blaschke, "Das Verfahren Der Feldorientierung Zur Regelung Der Asynchronmaschine", Siemens Forschungs-und Entwicklungsberichte 1, 1972.

[12] K. Hasse, "'Zur dynamik drehzahlgeregelter antriebe mit stromrichtergespeisten asynchrony-kurzschlublaufenn- aschinen", Darmstadt, Techn. Hochsch., Diss., 1969.

[13] Rupprecht Gabriel. Werner Leonhard, and Craig J. Nordby, “Field-Oriented Control of a Standard AC Motor Using Microprocessors”, *IEEE Transactions On Industrial Applications* vol. ia-16, no. 2, march/april 1980.

[14] Takayoshi Matsuo and Thomas A. Lipo, “A Rotor Parameter Identification Scheme forVector-Controlled Induction Motor Drives”, *IEEE Transactions On Industry Applications*, vol. ia-21, no. 4, may/june 1985.

[15] David M. Brod, and Donald W. Novotny, “Current Control of VSI-PWM Inverters”, *IEEE Transactions On Industry Applications*, vol. ia-21. no. 4, may/june 1985.

[16] Masato Koyama, Masao Yano, Isao Kamiyama, And Sadanari Yano, “Microprocessor-Based Vector Control System For Induction Motor Drives With Rotor

Time Constant Identification Function", *IEEE Transactions on Industry Applications*, vol. ia-22, no. 3, may/june 1986.

[17] Isao Takahashi, and Toshihiko Noguchi, "A New Quick-Response and High-Efficiency Control Strategy of an Induction Motor", *IEEE Transactions on Industry Applications*, vol. ia-22, no. 5. september/october 1986.

[18] Isao Takahashi, Member IEEE, Youichi Ohmori, "High-Performance Direct Torque Control Of An Induction Motor, *IEEE Transactions On Industry Applications*", vol. 25, no. 2, march/april 1989.

[19] Toshiaki Murata, Takeshi Tsuchiya, I Kuo Takeda, "Vector Control For Induction Machine On The Application Of Optimal Control Theory", *IEEE Transactions On Industrial Electronics*, Vol. 31, No. 4, August 1990.

[20] Marian P. Kazmierkowski And Waldemar Sulkowski, "A Novel Vector Control Scheme For Transistor PWM Inverter-Fed Induction Motor Drive*"*, *IEEE Transactions On Industrial Electronics*, vol. 38, no. 1, february 1991.

[21] N. Mohan, T. M. Undeland, and W. P. Robins, "Power Electronics: Converters Applications and Design", New York Wiley, 1989.

[22] A. Ekstrom, 'Calculation of transfer function for a forced commutated voltage-source inverter", in *Proc. IEEE PESC.*

[23] H. Mogi, M. Yabumoto, M. Mizokami, and Y. Okazaki, "Harmonic analysis of AC magnetostriction measurements under non-sinusoidal excitation", *IEEE Tram. On Magnetics*, vol. 32, no. ***5,*** pp. 491 1-4913, 1996.

[24] N. R. Zargari, P. Joos, and P. D. Ziogas, A performance comparison of PWM rectifiers and synchronous link converters", in *1171. ConJ Power Electronics and Motion Control*, pp. 346-35 1, 1992.

[25] J. Holtz, "Pulse width modulation - A Survey", *IEEE Trans. Industrial Elec*., Vol. 39, No. 5, pp. 4 10-420, Dec. 1992.

[26] J. K. Steinke, "Control Strategy for a three phase AC Traction drive with three-level GTO PWM inverter", *PESC Record*, pp. 431-438, 1988.

[27] T. Tohama, T. Kikuchi, K. Ishii, "3-LevelilCBT Inverter Propulsion Control System", *Japanese Railway Engineering*, pp. 330-337, 1991. NO. 130, pp. 10- 13, July 1994.

[28] Bimal K. Bose, Nitin R. Patel, and Kaushik Rajashekara "A Neuro–Fuzzy-Based On-Line Efficiency Optimization Control of a Stator Flux-Oriented Direct Vector-Controlled Induction Motor Drive", *IEEE Transactions On Industrial Electronics,* vol. 44, no. 2, april 1997.

[29] James N. Nash, "Direct Torque Control, Induction Motor Vector Control without An Encoder", *IEEE Transactions On Industry Applications*, vol. 33, no. 2, march/april 1997.

[30] Bimal K. Bose, Nitin R. Patel, And Kaushik Rajashekara, "A Start-Up Method For A Speed Sensorless Stator-Flux- Oriented Vector-Controlled Induction Motor Drive", *IEEE Transactions on Industrial Electronics*, vol. 44, no. 4, august 1997.

[31] Emanuele Cerruto, Alfio Consoli, Angelo Raciti, and Antonio Testa, "Fuzzy Adaptive Vector Control Of Induction Motor Drives", *IEEE Transactions On Power Electronics*, vol. 12, no. 6, november 1997.

[32] Yi-Hwa Liu, Chern-Lin Chen, and Rong-Jie Tu, "A Novel Space-Vector Current Regulation Scheme For A Field-Oriented-Controlled Induction Motor Drive", *IEEE Transactions On Industrial Electronics*, vol. 45, no. 5, october 1998.

[33] Cyril W. Lander-"Power Electronics", McGraw-Hill Book Company.

[34] Bimal. K.Bose – "Modern Power Electronics & AC Drives", Prentice Hall.